EXHIBIT A180

The Canadian Mineralogist
Vol. 54, pp. 1403-1435 (2016)
DOI: 10.3749/canmin.1500109

AMPHIBOLE DUSTS: FIBERS, FRAGMENTS, AND MESOTHELIOMA

ANN G. WYLIE[§]

Laboratory for Mineral Deposits Research, Department of Geology, University of Maryland, College Park, Maryland 20742, USA

ABSTRACT

Thirty-one sets of data containing lengths and widths of micron- and submicron-sized particles of amphibole asbestos fibers and fragmented amphibole particles and four sets containing summary data are compared in this study. The goals are to describe characteristics of amphibole asbestos fiber populations across asbestos occurrences, to determine which correlate most closely with the generally accepted relative risks for mesothelioma, and to describe the characteristics of amphibole cleavage fragment populations for which an excess risk for mesothelioma has not been established. The analysis shows that modal widths of asbestos fibers vary among geologic occurrences, many asbestos dust populations display multimodal widths, the modes occur at different widths, and the tendency for fibers to disaggregate into component fibrils varies. It also shows that all exposures associated with elevated mesothelioma contain abundant fibers >5 μm in length that have widths <0.25 μm, including fibers <0.15 μm, and that risk for mesothelioma qualitatively corresponds to their abundances. Other parameters that might serve as proxies to correlate with relative risk include fibers with $L > 5$ μm and $W \leq 0.33$ μm and $L > 10$ μm and $W \leq 0.33$ μm. Such particles are absent or occur only in trace amounts in amphibole cleavage fragment populations. Asbestos fibers with such small widths are, for the most part, excluded from occupational exposure assessments which rely on optical microscopy or transmission electron microscopy (TEM) equivalents, compounding the already difficult assessment of risk from inhalation of elongated amphibole particles in a mixed dust environment, especially mining. If we are to understand the outcomes of occupational exposures and the responses observed in animal and cell culture experimentation, the abundance and characteristics of the narrowest elongated mineral particles in the exposure should be established by electron microscopy.

Keywords: amphibole, asbestos, cleavage fragments, mesothelioma, particle dimensions.

INTRODUCTION

Asbestos is a term applied to a group of highly fibrous members of the amphibole and serpentine group of minerals that formed as high tensile-strength fibers, which have been mined for their unique physical and chemical properties. Recent reviews include Veblen & Wylie (1993) Skinner *et al.* (1988) and Dorling & Zussman (1987). Asbestos fibers are easily separable by hand pressure into smaller fibers due to a fibrillar growth habit in which individual single or twinned crystals of very small width, called fibrils, share a common axis of elongation (the c-axis in amphiboles) but are randomly distributed around that axis with respect to the other crystallographic directions. The fibrillar structure results in anomalous optical properties (Verkouteren & Wylie 2002). Fibril lengths may exceed a hundred micrometers and fibrils with widths less than 0.25 μm are common in asbestos ores. The high aspect ratio of these fine fibrils and bundles of fibrils enhances their flexibility and tensile strength with the narrowest fibrils displaying the highest tensile strength (Walker & Zoltai 1979).

Asbestos is well-established as a causal agent in malignant diseases, notably mesothelioma and lung cancer, and in nonmalignant lung fibrosis (asbestosis). Although mining of asbestos has ceased in most places in the world, asbestos remains in the environment as a component of some metamorphosed magnesium-rich and carbonate rocks and the soils derived from them (Wylie & Candela 2015). It is also in place in many buildings around the world. Therefore, it will remain a societal concern for years to come.

[§] *Corresponding author e-mail address*: awylie@umd.edu

High incidences of mesothelioma occur following occupational exposure to some asbestos. Regulatory permissible exposure limits (PEL) for asbestos are based on dose-response relationships for mesothelioma among those occupationally exposed, primarily to crocidolite. Elevated occurrences of mesothelioma have also been reported from exposure to dusts containing asbestiform amphibole not mined as asbestos, including asbestiform tremolite, winchite, richterite, and fluoro-edenite (McDonald *et al.* 1986, Amandus *et al.* 1987, Paoletti *et al.* 2000, Sullivan 2007, Constantopoulos 2008, Yaziciogly *et al.* 1980, Sakellariou *et al.* 1996).

The specific modes of action of the various types of asbestos in the development of asbestos-related diseases remain unknown, but both modes of action and potencies differ among asbestos from different locations (Mossman *et al.* 2011, Cyphert *et al.* 2012, Berman & Crump 2008, 2003, Lippmann 2014). For example, amphibole asbestos is generally recognized as a more potent carcinogen than chrysotile (Pooley & Wagner 1988, Case *et al.* 2011, Lippmann 2014). In their review of occupational experiences, Hodgson & Darnton (2000) calculated the relative risks for developing mesothelioma risks from exposure to amosite[1] and crocidolite[2] as 100:500. Carbone *et al.* (2012) estimated that the risk for mesothelioma for miners of amosite is an order of magnitude lower than for miners of crocidolite. White *et al.* (2008) reviewed environmental mesotheliomas in South Africa and concluded that crocidolite is far more mesotheliomagenic than amosite. The relative risk for mesothelioma is lowest for anthophyllite asbestos from Finland, as only a few cases among those occupationally exposed have been reported (Lippmann 2014).

The unusual dimensions of asbestos fibers have been known to be a significant factor in asbestos-related diseases since the seminal animal experiments of Stanton *et al.* (1981), who introduced the idea that the only criteria for the carcinogenicity of a mineral fibers is that they be durable in the lung and be of a certain size. Based on this work and other animal studies that followed, many dimensional criteria for "most carcinogenic" durable mineral fibers have been proposed (*e.g.*, Pott 1978, Berman & Crump 2003). Timbrell *et al.* (1971) called on narrower widths to explain the higher incidence of mesothelioma and asbestosis among Cape crocidolite miners and millers than among miners and millers of amosite or crocidolite from the Transvaal region of South Africa. Timbrell (1983) argued that the smaller number of mesothelioma cases associated with exposure to anthophyllite asbestos from Paakkila compared to exposure to Cape crocidolite makes a width of about 0.1 μm the width threshold needed to produce mesothelioma in humans. Lippmann (2014), in his comprehensive review of the relationship between carcinogenicity and dimensions, agreed with Timbrell and affirmed his earlier proposal that mesothelioma is produced by bio-persistent fibers with $L \geq 5$ μm, $W \leq 0.15$ μm; these fibers can readily penetrate the deepest reaches of the lung and pleura with a high likelihood of being retained, and for this reason they represent the greatest hazard for mesothelioma.

Estimates of the dimensions of fibers that can access the pleura are based on lung geometry, biological processes, and analysis of tissue. In a literature review, Lentz *et al.* (2003) concluded that fibers <0.4 μm in width may more readily translocate to the pleura. The data from Paoletti & Bruni (2009) support the idea that narrow fibers are more readily transported to the pleura. Carbone *et al.* (2012) in their review on this topic report that fibers <0.3 μm in width are concentrated in the pleura. Width means and modes and their relation to carcinogenicity were reviewed by Wylie *et al.* (1993). While width may be a major factor in controlling the translocation of fibers from the lung to the pleura, it may also be important in other ways. It has been shown that the rate and direction of cellular movement can be controlled by nanoscale topographic features and that the effects extend to features on the scale of a few hundred nanometers, the size of the smallest fibrils (Driscoll *et al.* 2014, Sun *et al.* 2015).

---

[1] Amosite is a commercial term derived from Asbestos Mines of South Africa, located in the Pietersburg Asbestos Field, Limpopo Province, and Transvaal, South Africa. It is not a proper mineralogical term. It is formed primarily of the mineral grunerite, but very small amounts of anthophyllite and actinolite have been reported in mine products. Data sets may or may not differentiate among these minerals. For that reason, because all amosite in commerce comes from the Transvaal, and because of its widespread use among biologists, epidemiologists, public health workers, and regulatory bodies, the term amosite is used in this paper.

[2] Crocidolite is the now-discouraged variety name for riebeckite asbestos, notably from Hammersley Range, Australia; Northern Cape Asbestos Field, Northern and North West Cape Provinces, South Africa, referred to as Cape crocidolite; the Pietersburg Asbestos Field, South Africa (Limpopo Province), referred to as Transvaal crocidolite; and Bolivia. It is used in this paper because of its widespread use among biologists, epidemiologists, public health workers, and regulatory bodies.

Fibers shorter than 5 μm are abundant in all exposures. Suzuki & Yuen (2002) showed that despite the body's ability to remove short fibers preferentially, approximately 50% of the amphibole particles found in lung tissue from 168 cases of mesothelioma were less than 5 μm in length, and studies of length distributions of airborne and bulk samples clearly indicate that the overwhelming majority of fibers are less than 5 μm in length (Wylie 1993). Pooley & Clark's (1980) analysis of the lung burden of asbestos among mesothelioma cases in miners yielded 76.6% of crocidolite and 60% of amosite fibers shorter than 4 μm. Overall, short fibers provide the highest portion of surface area in an asbestos dust cloud and surface area has been shown to accelerate inflammation and lung damage and to correlate with fibrosis (asbestosis) (Timbrell *et al.* 1988). Dodson *et al.* (2003) argued that fibers of all lengths induce pathological responses and caution should be used in excluding any portion of the inhaled fiber population.

It is generally agreed that not only is the toxicity of asbestos related to the width, length, and effective surface area, but crystallinity, surface chemistry, and reactivity are also factors that may need to be considered in understanding the pathogenicity of asbestos (Hochella 1993, Lower *et al.* 2000). Wagner *et al.* (1985) concluded that the carcinogenicity of (wooly) erionite in rats was much greater than could be predicted based on dimensions alone. The iron content of amphiboles may be relevant to their toxicity because it can generate highly toxic and potentially mutagenic reactive oxygen species (Aust *et al.* 2011 and Huang *et al.* 2011). Carbone *et al.* (2012) review the evidence for the role of genetic predisposition and exposure to co-factors in disease production, arguing that otherwise, based on exposure alone, more than the observed 4.7% of asbestos miners would have developed mesothelioma. The mesothelioma experienced by occupational exposure to chrysotile is widely believed to be explained by tremolite asbestos contamination of Canadian chrysotile (Lippmann 2014), primarily because chrysotile is soluble in lung fluids (Hume & Rimstidt 1992).

Uncertainties about the carcinogenic potency of elongated particles that are not asbestos fibers have been expressed by the U.S. National Institute of Occupational Safety and Health (NIOSH), through their introduction of the term "elongated mineral particle" (EMP), which they define as any particle possessing as aspect ratio (length/width) of at least 3 (NIOSH 2011). In a regulatory context, EMP refers only to elongated particles longer than 5 μm; in this paper it refers to any particle with aspect ratio of at least 3. When crushed, common amphibole fragments form particles referred to as cleavage fragments, which are shaped by two directions of perfect cleavage parallel to the **c**-axis and are therefore elongated. Parting in amphiboles is normally parallel to the **c**-axis, and, when present, will accentuate elongation. Many amphibole cleavage fragments meet the definition of EMPs, especially those longer than 5 μm, because aspect ratio increases with length (Siegrist & Wylie 1980).

In their roadmap for research, NIOSH frames a research agenda that addresses the questions, do all durable EMPS have a significant carcinogenic potential, and if so, how does the magnitude of this potential vary among mineral exposures? They discuss the role of chemical, physical, morphological, dimensional, and surface characteristics of airborne EMPs in determining carcinogenic potential, in particular those that result in positive associations with mesothelioma. In doing so, they open the question of the carcinogenic potential of any durable EMP longer than 5 μm that can be inhaled, independent of its mineralogy. For most silicates, a width of about 3.5 μm approaches the limit of respirability (Timbrell 1965), and airborne cleavage fragments are often of this size. However, respirability does not necessarily equate with carcinogenicity. There is strong evidence that respirable amphibole cleavage fragments (both EMPs and non EMPs) are non-mesotheliomagenic (Addison & McConnell 2008, Gamble & Gibbs 2008, Williams *et al.* 2012), and they have also generally proven nonpathogenic in animal studies and *in vitro* studies, suggesting that cleavage fragments are less bioreactive and cytotoxic than asbestos (Mossman 2008). The studies reported by Mossman, however, lack details on particle sizes necessary to evaluate their relevance to the relationship between amphibole dimensions and mesotheliomagenic potential. More detail on the dimensions that correlate with mesothelioma incidence is needed.

Purpose of the Paper

Despite what we have learned in studying asbestos exposures and disease outcome, determining which population characteristics equate with carcinogenic potential remains an issue both for understanding the mode of action of asbestos in lung disease and for the regulatory community who need clear guidelines to protect public health. One goal of this paper is to evaluate dimensional characteristics of asbestiform amphiboles to see what can be learned about fibrils and the fibrillar structure of asbestos and of asbestiform amphiboles, how the amphibole habit is reflected in an aerosol, how habit affects regulatory exposure assessment, how habits vary among occurrences of asbestos, including the tendency for fibers to disaggregate into

component fibrils, and how these variations may impact our understanding of asbestos and asbestos-related disease.

In order to monitor airborne particles for asbestos or identify asbestos in rock containing massive amphibole crushed for consumer products (*e.g.*, crushed stone, vermiculite, wollastonite, and talc), dimensional analysis is one of only a few tools we have to measure the exposure to asbestos. Therefore, another goal of this study is to determine if a discriminating tool based on EMP dimensions can be found that would readily separate airborne amphibole populations by habit and perhaps, by carcinogenicity.

The study will also address the concerns expressed by Lippmann (2014) that there is inadequate data for amphiboles from the vermiculite deposit at Libby, Montana. Four of the data sets are from Libby. The frequency distributions of length and width, and associated tables included in this paper, will provide a resource for those interested in the pathogenicity of amphibole asbestos and common amphibole.

Data Sources

The 35 data set studies are described in Table 1. All were collected as part of health-related studies. Measurements were manual, and fiber measurements were recorded in discrete intervals. A few of the data sets contain only summary data expressed as percentages in specific length and width intervals, but they are included because they provide data on aerosolized amosite and crocidolite in the mining environment, for which raw data sets are not available. Details of the sample preparation and measurement protocols can be found in the references provided with each data set.

Asbestos populations were derived from raw fibers, fibers found in lung tissue, fibers isolated by settling in water, and fibers collected on air monitoring filters in occupational environments. While lung and pleura burden characteristics are usually the best determinant for disease relationships, as these data show, they are closely related to the aerosol and to samples prepared to approximate the aerosol.

Data sets came from major asbestos deposits (Cape crocidolite, Transvaal amosite) whose association with elevated mesothelioma is well documented, and from Libby, Montana, where asbestiform Na-Ca amphiboles (dominated by winchite) are known carcinogens. They include tremolite-asbestos from Korea and India and actinolite asbestos from Africa and Virginia. Among them are samples used for National Institute of Standards and Technology (NIST) Standard Reference Materials (SRM) for actinolite asbestos, tremolite asbestos, crocidolite asbestos and amosite, and samples of crocidolite, amosite, and tremolite cleavage fragments prepared for the National Institute of Environment Health Sciences (NIEHS) as reference materials.

There are a few notable absences from the asbestos populations: anthophyllite asbestos from Paakkila, Finland, and crocidolite from Australia. However, summary data for both of these deposits have been published and are included in Table 2.

The data for common amphibole cleavage-fragment EMPs are from crushed samples from Colorado, Canada, Sweden, South Dakota, California, and New York, from airborne amphibole particles from three mining operations, and from ambient dusts from El Dorado Hills, California. Protocols for selecting particles for measurement vary significantly among the data sets. At two mining sites, Homestake Mine in South Dakota and Peter Mitchell Pit in Minnesota, epidemiological studies have been conducted. No measurements of lung-burden cleavage fragments are available.

The comparisons in this study are based only on EMPs; all other particles have been removed from the populations analyzed. Comparisons among populations that are not EMPs were not considered because some data sets exclude them or apply other criteria for counting, such as minimum length or other aspect ratio, which impact differently the proportion of EMPs in the population. The number of EMPs and non-EMPs in the data sets are included in Table 1.

Both TEM and SEM were used to gather data (specified in Table 1). Ten data sets were collected with a single set of experimental conditions at the research laboratories of the U.S. Bureau of Mines in College Park, Maryland, later Avondale, Maryland, with SEM. Ten were collected following a different protocol at Research Triangle Institute (RTI), North Carolina, with TEM. There are also data sets from other laboratories using TEM. Data sets are identified by the letter designation given in Table 1 (*e.g.*, A, B, *etc.*) in figures, tables, and text.

Methods

Frequency distributions of width were constructed using bin intervals of 0.06 to 0.127 μm as specified in Table 1; frequencies are expressed as % per bin interval. The precision of measurements, if known, is equal to half the bin interval. By considering bin selection carefully and keeping bin intervals small, fluctuations in frequencies of width on the scale of the unit fibrils can be seen. Width frequencies are presented for EMPs longer and shorter than 5 μm. A 5 μm length was chosen because it can be used as a rough measure of likelihood of retention once inhaled, it is used commonly as the criterion to separate "long"

and "short" fibers (and this terminology is followed in this paper), and it is part of the definition of a fiber employed in exposure monitoring for regulatory compliance. Frequency distributions of length are expressed as % per μm. In addition to presenting frequency of width for EMPs with $L > 5$ and $L \leq 5$ μm, tables providing width mean, mode, and range for length intervals 1–5, 5–10, 10–15, and >15 μm are also included (Tables 3–7). A unified approach to the analysis of multiple data sets facilitates comparisons among them.

The populations are compared in terms of EMP percentages in specific length and width categories in Table 8. The optical microscope protocol for occupational monitoring limits visibility to about 0.25 μm. Those TEM methods that are designed to compare to optical measurements by convention use 0.25 μm as a minimum width for exposure assessment. The proportion of EMPs <0.25 μm in width and >5 μm in length approximates the proportion excluded in occupational monitoring. The proportion of EMPs >5 μm that have width ≤0.33 μm is a proxy for the size of particles preferentially transported to the pleura, and a width of ≤0.5 μm was used since it is a convenient and frequently used measure of "thin" EMPs. The proportion of EMPs >10 μm that have widths ≤0.33 μm is a proxy for the abundance of long EMPS that are also very thin.

Samples from which some of the data sets were derived or samples from the same location were examined by polarized light microscopy to determine extinction angles. Parallel extinction or anomalously small extinction angles and near uniaxial optical properties for monoclinic amphiboles is indicative of a fibrillar fiber structure with fibrils less than about 0.2 μm in size. Parallel extinction may also develop from polysynthetic twinning on {100} (Wylie 1979, Verkouteren & Wylie 2002). Where available, observations of optical properties are included.

Results

Crocidolite

Figure 1a shows the frequency distributions of width of airborne and lungburden crocidolite EMPs from the Northern Cape Asbestos Field, South Africa, the most important world source of commercially mined crocidolite. The distinctive characteristic of Cape crocidolite is the uniform, narrow width of its fibers. A high proportion of fibers with modal width of ≈0.1 μm, and preponderance of fibers with width <0.3 μm, are found in all airborne dusts and are characteristic of fibers of all lengths (Fig. 1a). These tiny widths account for the high tensile strength of crocidolite (Walker & Zoltai 1979) and explain its invariant parallel extinction. The ranges of length of the populations are shown in Figure 1c. They too are quite uniform, with the vast majority of fibers shorter than 5 μm.

The frequency of width and length measured from bulk samples of the NIEHS crocidolite and the raw-NIST SRM crocidolite are shown in Figures 1b and 1c. The NIEHS materials were characterized by Campbell *et al.* (1980) for animal-feed studies and the NIST SMRs were characterized by the Research Triangle Institute for NIST (Harper *et al.* 2008); they are therefore referred to as NIEHS and raw-NIST SRMs. Both display unimodal distributions of width centered at about 0.2 μm, significantly larger than airborne and lung-burden fibers; the range in width and length and the modal length are also much greater in these populations. The fibers ≤5 μm in length are much more abundant in population C than E. Population C was characterized by TEM and E was characterized by SEM.

Width range, mean, and mode for specific length intervals of Cape crocidolite populations are provided in Table 3. The data show the uniform nature of width for fibers of all lengths, with only slight increase in the mode for the longest fiber bundles; the narrowest fibers measured occur in all length segments. Shedd (1985) reports smaller mean fibril widths from the Cape (Table 2) than presented here. This may be due to her measurements being made with a higher-magnification TEM or to a protocol that resulted in greater disaggregation of the component fibrils prior to measurement.

The frequency of width of crocidolite fibers from Wittenoon, Australia, was determined by Shedd (1985) from bulk samples and by Timbrell *et al.* (1988) from lung burden. Timbrell *et al.* (1988) concluded that Wittenoon crocidolite fibrils are slightly narrower than fibrils from the Cape, but Shedd (1985) indicates that they are remarkably similar (Table 2). It may be the case that the differences between these two studies reflect the fact that narrower fibers have a higher probability of becoming airborne and being deposited and retained in the lung rather than a real difference in the width of the smallest fibrils.

Shedd's (1985) frequency distributions for width for Cape and Australian crocidolites are bimodal. The measurements Shedd (1985) reports have a precision of ±0.01, much greater than other data sets in this paper, enabling a detailed look at the widths of the narrowest fibrils. For all lengths of Cape and Australian crocidolite, modes of 0.05–0.075 μm and at 0.1–0.2 μm were observed by Shedd (1985), although slightly smaller modes were found in a few. High-precision measurement of widths of crocidolite found in lung tissue of mesothelioma cases has also

TABLE 1. DATA SETS

A. RIEBECKITE, CA. Nonfibrous mineral specimen from Long Valley Creek Quarry, California, from the U.S. National Museum (No. R119931). The sample was ground, dispersed in water, and filtered, and particles were measured by SEM. Details on sample preparation, publication of prior analyses, and the raw data can be found in Wylie *et al.* (2015). Frequency of width is based on a bin interval of 0.110 μm. $N = 968$, N EMP = 651, N EMP >5 μm = 402.

B. RIEBECKITE, CO. A nonfibrous mineral sample reported by Harper *et al.* (2008) to come from St. Peter's Dome, Colorado. The measurements were made by TEM at Research Triangle Institute (RTI) from crushed and ground material which was dispersed in water and then selectively sampled by settling velocity to maximize those particles >5 μm in length (L), <3 μm in width (W), and with a length-to-width or aspect ratio (AR) of >3:1 (Harper *et al.* 2008). The data are taken from Beard *et al.* (2007) and were provided in electronic form by the National Institute of Occupational Safety and Health. Frequency of width is based on a bin interval of 0.127 μm. $N = 300$, N EMP = 195, N EMP >5 μm = 60.

C. NIEHS CROCIDOLITE, SA. Asbestos from the Kuruman Hills of South Africa, from a mine located near the Kalahari Desert, Northern Cape Province. The particle measurements were made for the National Institute of Environmental Health Sciences (NIEHS) (Campbell *et al.* 1980). Preparation included jet milling to break bundles, dispersal in water, and filtration. Measurements were made with an SEM. Details of sample preparation, publication of prior analyses, and the raw data can be found in Wylie & Virta (2016b). Frequency of width is based on a bin interval of 0.110 μm. $N = 1038$, N EMP = 1030, N EMP >5 μm = 497.

D. AIRBORNE CROCIDOLITE [D(a)] and CROCIDOLITE, LUNG BURDEN [D(b)]. Frequencies of length and width of crocidolite extracted from lung tissue of mesothelioma and asbestosis patients and collected by open-face sampling of airborne crocidolite at the Pomfret Mine, Cape Province, South Africa are taken from Pooley & Clark (1980). Frequency of width is based on a bin interval of 0.125 μm. Data were expressed only as percentages in particular length and width categories; no N provided. By assuming that the length range of 4–6 μm is equally split between > and <5 μm, the proportion >5 μm is estimated to be 17% for crocidolite from lung tissue and 11% for airborne crocidolite.

E. CROCIDOLITE, raw-NIST SRM. This is a mine product from the Cape Province of South Africa. It was sent by RTI to the National Institute of Standards and Technology (NIST) for a NIST Standard Reference Material (SRM). The measurements were obtained by TEM from material retained by RTI. The asbestos was dispersed in water and then selectively sampled by settling velocity to maximize those particles L >5 μm, W <3 μm, and AR >3:1 (Harper *et al.* 2008). Measurements were made following procedures described in Beard *et al.* (2007). The data were provided in electronic form by the National Institute of Occupational Safety and Health. Frequency of width is based on a bin interval of 0.120 μm. $N = 300$, N EMP = 300, N EMP >5 μm = 231.

F. AIRBORNE CROCIDOLITE. Airborne particles were collected from working areas described as mining [F(a)] and bagging in the mill [F(b)] of the Cape Province asbestos mines, South Africa, and analyzed using TEM by Gibbs & Hwang (1980). Data are restricted to EMPs and are expressed as percentages in particular length and width categories. N is not provided. Frequency of width is based on a bin interval of 0.060 μm. Percentage of EMPs >5 μm is 4% for mining and 7% for bagging.

G. AIRBORNE CUMMINGTONITE–GRUNERITE, SD. Grunerite particles from air monitoring filters from the Homestake Mine, South Dakota. Filters were sent to the U.S. Bureau of Mines from the U.S. Mine, Safety and Health Administration in about 1977. Details of sample preparation, prior publication, and the raw data can be found in Wylie *et al.* (2015). Particles were dispersed, filtered, and studied by SEM. Frequency of width is based on a bin interval of 0.110 μm. $N = 501$, N EMP = 361, N EMP >5 μm = 160.

H. CUMMINGTONITE–GRUNERITE, SD. This non-fibrous sample of the cummingtonite–grunerite mineral series comes from Homestake Mine, South Dakota. It was purchased by Harper *et al.* (2008) as cummingtonite but is referred to here as cummingtonite–grunerite since its Mg/(Mg + Fe) is unknown. The measurements were made by TEM from crushed and ground material which was dispersed in water and then selectively sampled by settling velocity to maximize those particles with L >5 μm, W <3 μm, AR >3:1 (Harper *et al.* 2008). The data are taken from Beard *et al.* (2007) and were provided in electronic form by the National Institute of Occupational Safety and Health. Frequency of width is based on a bin interval of 0.127 μm. $N = 300$, N EMP = 210, and N EMP >5 μm = 57.

TABLE 1. CONTINUED.

I. GRUNERITE. The data are for a nonfibrous member of the cummingtonite–grunerite series from Tras os Montes, Portugal (Harper *et al.* 2008). Data from Beard *et al.* (2007) indicate that the Mg content is very low and grunerite is the appropriate name for the mineral. The measurements were made by TEM using crushed and ground material which was dispersed in water and then selectively sampled by settling velocity to maximize those particles with L >5 μm, W <3 μm, AR >3:1 (Harper *et al.* 2008). The data are taken from Beard *et al.* (2007) and were provided in electronic form by the National Institute of Occupational Safety and Health. Frequency of width is based on a bin interval of 0.121 μm. *N* = 300, *N* EMP = 209, *N* EMP >5 μm = 35.

J. AIRBORNE GRUNERITE and ACTINOLITE, MN. Grunerite and some actinolite particles from air monitoring filters from Peter Mitchell Pit, Reserve Mine, Minnesota. Filters were sent to the U.S. Bureau of Mines from the U.S. Mine, Safety and Health Administration in about 1977. Details of sample preparation, publication of prior analyses, and the raw data can be found in Wylie *et al.* (2015). Particles were dispersed, filtered, and studied by SEM. Frequency of width is based on a bin interval of 0.110 μm. *N* = 1113, *N* EMP = 86, *N* EMP >5 μm = 28.

K. NIEHS AMOSITE. The asbestos, characterized for the NIEHS, is from the Transvaal from a mine near Penge, Limpopo, South Africa (Campbell *et al.* 1980). It is called amosite after its source, Asbestos Mines of South Africa. Normally considered to be synonymous with grunerite-asbestos, NIEHS amosite is composed of 95% grunerite asbestos and 5% actinolite asbestos. Preparation included jet milling to break bundles, dispersal in water, and filtration. It was studied by SEM. Details of sample preparation, publication of prior analyses, and the raw data can be found in Wylie & Virta (2016). Frequency of width is based on a bin interval of 0.110 μm. *N* = 1024, *N* EMP = 1015, *N* EMP >5 μm =802.

L. AIRBORNE AMOSITE – SHIPYARD. Amosite particles collected from air monitoring of a shipyard where amosite was in use were measured. The filters were sent by OSHA to the U.S. Bureau of Mines in 1979. Details of sample preparation, publication of prior analyses, and the raw data can be found in Wylie *et al.* (2015). Particles were dispersed, filtered, and studied by SEM. Frequency of width is based on a bin interval of 0.110 μm. *N* = 839, *N* EMP = 837, *N* EMP >5 μm = 429.

M. AIRBORNE AMOSITE – ELECTRICAL. Amosite particles were collected from air monitoring of an electric company where amosite was in use. The filters were sent by OSHA to the U.S. Bureau of Mines in 1979. Details of sample preparation, publication of prior analyses, and the raw data itself can be found Wylie *et al.* (2015). Particles were dispersed, filtered, and studied by SEM. Frequency of width is based on a bin interval of 0.110 μm. *N* = 374, *N* EMP = 374, *N* EMP >5 μm. = 284.

N. AIRBORNE AMOSITE [N(a)] and AMOSITE LUNG BURDEN [N(b)]. Frequencies of length and width of amosite extracted from the lung tissue of mesothelioma and asbestosis patients and collected by open-face sampling of airborne amosite at the Penge Mine in South Africa are taken from Pooley & Clark (1980). Measurements are by TEM. Frequency of width is based on a bin interval of 0.125 μm. All data were given in percentages; no *N* provided. By assuming that the length range 4–6 μm is equally split between > and <5 μm, the proportion >5 μm is estimated to be 31% for amosite from lung tissue and 25% for airborne crocidolite.

O. AIRBORNE AMOSITE. Airborne particles were collected in working areas described as mining [O(a)] and bagging [O(b)], Transvaal asbestos mines, South Africa, and were analyzed by TEM (Gibbs & Hwang 1980). All data are for EMPs and are expressed as percentages in particular length and width categories. Frequency of width is based on a bin interval of 0.060 μm. *N* is not provided. Percentage >5 μm is given as 12% for mining and 25% for bagging.

P. AMOSITE, Raw-NIST SRM. Asbestos from the Transvaal, South Africa, from the original material sent to NIST by RTI that was later to become a NIST SRM. The measurements were made by TEM from crushed and ground material which was dispersed in water and then selectively sampled by settling velocity to maximize those particles L >5 μm, W <3 μm, and AR >3:1 (Harper *et al.* 2008). The data are from Beard *et al.* (2007) and were provided in electronic form by the National Institute of Occupational Safety and Health. Frequency of width is based on a bin interval of 0.120 μm. *N* = 300, *N* EMP = 292, *N* EMP >5 μm = 143.

Q. TREMOLITE NY NIEHS (1). Tremolite from Vanderbilt Mine, Balmat, New York, was milled, dispersed in water, and measured by SEM. This nonfibrous tremolite was characterized for the NIEHS and is labeled Tremolite (NIEHS) (Campbell *et al.* 1980). Optical properties and composition are given by Verkouteren & Wylie (2000) (sample number 247). Frequency of width is based on a bin interval of 0.110 μm. Details of sample preparation, prior publication of analyses, and the raw data can be found in Wylie & Virta (2016b). *N* = 617, *N* EMP = 157, *N* EMP >5 μm = 65.

TABLE 1. CONTINUED.

R. TREMOLITE, NY NIEHS (2). The NIEHS tremolite from NY was analyzed at RTI by TEM. The data are taken from Beard *et al.* (2007) and were provided in electronic form by the National Institute of Occupational Safety and Health. The measurements were made by TEM using material ground by mortar and pestle, dispersed in water, and allowed to settle to maximize those particles with L >5 μm, W <3 μm, and AR >3:1 (Harper *et al.* 2008). Frequency of width is based on a bin interval of 0.121 μm. *N* = 300, *N* EMP = 233, *N* EMP >5 μm = 48.

S. TREMOLITE, CA $PM_{2.5}$. The tremolite data are from Cyphert *et al.* (2012). Tremolite was collected from the south shore of Folsom Lake, near El Dorado Hills, California. It was crushed and ground and subject to water elutriation to isolate respirable particles with aerodynamic diameters of less than 2.5 μm. Measurements were made by TEM. Frequency of width is based on a bin interval of 0.110 μm. *N* = 296, *N* EMP = 113, EMP >5 μm = 3.

T. ACTINOLITE, CA. This non-fibrous sample of actinolite comes from San Bernardino County, California, near Wrightwood. The measurements were made by TEM from crushed and ground material which was dispersed in water and then selectively sampled by settling velocity to maximize those particles with L >5 μm, W <3 μm, and AR >3:1 (Harper *et al.* 2008). The data are taken from Beard *et al.* (2007) and were provided in electronic form by the National Institute of Occupational Safety and Health. Frequency of width is based on a bin interval of 0.121 μm. *N* = 300, *N* EMP = 231, *N* EMP >5 μm = 34.

U. AIRBORNE ACTINOLITE, VA. Air-monitoring filters from Shadwell Quarry, Charlottesville VA, were sent to the U.S. Bureau of Mines from the U.S. Mine, Safety and Health Administration in about 1977. The particles were dispersed, filtered, and studied by SEM. Details of sample preparation, publication of prior analyses, and the raw data itself can be found in Wylie *et al.* (2015). Frequency of width is based on a bin interval of 0.110 μm. *N* = 613, *N* EMP = 427, *N* EMP >5 μm = 183.

V. AIRBORNE TREMOLITE–ACTINOLITE and HORNBLENDE, CA. Amphibole particulate collected on air-monitoring filters during disturbed and undisturbed conditions around El Dorado Hills, California, were identified and measured by TEM by LabCor. Actinolite and/or hornblende is more common than tremolite in the data set. They have been described by EEI (2005). Data were provided by Rich Lee (*pers. commun.*). Frequency of width is based on a bin interval of 0.100 μm. *N* = 3947, *N* EMP = 3219, EMP >5 μm = 1655.

W. ACTINOLITE ASBESTOS var. MOUNTAIN LEATHER. Mineral specimen from the collection of the Bureau of Mines, location Africa. Mountain-leather actinolite is reported commonly from the metamorphosed mafic rock of the Appalachian, Cordilleran, and Alpine orogenic belts and from South Africa. It forms from weathering asbestos. The sample was ground lightly to separate fibers, dispersed in water, and filtered. Particles were measured by SEM. Details of sample preparation, prior publication of analyses, and the raw data are available from Wylie & Virta (2015a). Frequency of width is based on a bin interval of 0.110 μm. *N* = 624, *N* EMP = 521, *N* EMP >5 μm = 61.

X. TREMOLITE ASBESTOS, INDIA. The asbestos is from the Udiapur District, Rajasthan State, India. It was ground, dispersed in water, and filtered. Particles were measured by SEM. Details of sample preparation, prior publication of analyses, and the raw data are in Wylie & Virta (2016a). The material has also been described by Campbell *et al.* (1979) and Verkouteren & Wylie 2000 (sample 14). Frequency of width is based on a bin interval of 0.110 μm. *N* = 472, *N* EMP = 191, *N* EMP >5 μm = 37.

Y. TREMOLITE ASBESTOS, KOREA. This is commercially produced asbestos from Korea. Its optical properties are described by Verkoutern & Wylie (2000) (sample 144). It was dispersed in water and photographed by TEM, and measured from photographs. Frequency of width is based on a bin interval of 0.060 μm. *N* EMP = 1443, *N* EMP >5 μm = 655. Data are from Jennifer Verkouteren (*pers. commun.*).

Z. TREMOLITE ASBESTOS, CA. This material was sent to NIST by RTI to serve as the NIST SRM. It is from the Condo deposit, near Barstow, California. The NIST SRM description specifies that some of the fibers are loose, and other more tightly bound. A small amount of material may be massive. The measurements were made by TEM using the material retained by RTI that was dispersed in water and selectively sampled to maximize those particles with L >5 μm, W <3 μm, and AR >3:1 (Harper *et al.* 2008). The data are from Beard *et al.* (2007). They were provided in electronic form by the National Institute of Occupational Safety and Health. Frequency of width is based on a bin interval of 0.120 μm. *N* = 300, *N* EMP = 134, *N* EMP >5 μm = 432.

TABLE 1. CONTINUED.

AA. ACTINOLITE ASBESTOS NIST SRM. The material was sent to NIST by RTI to serve as the NIST SRM. The NIST data sheet states that some of the fibers are loose and others are more tightly bound together, and a considerable amount of material may be massive. The massive material contains significant clinochlore . It was collected from a construction site in Fairfax County, Virginia. The measurements were made by TEM from material retained by RTI, dispersed in water, and selectively sampled for particles with L >5 μm, W <3 μm, and AR >3:1 (Harper *et al.* 2008). The data are from Beard *et al.* (2007) were provided in electronic form by the National Institute of Occupational Safety and Health. Frequency of width is based on a bin interval of 0.120 μm. $N = 300$, N EMP = 233, N EMP >5 μm = 103.

BB. FERRO-ACTINOLITE ASBESTOS, SA. Ferro-actinolite asbestos from South Africa, probably from the Cape region, is from the museum collection of the U.S. Bureau of Mines, sample 03704. Optical properties and chemical composition can be found in Verkouteren & Wylie (2000, 2002) sample number 66. It is known by the variety name prieskite. Preparation included dispersal in water and filtration. It was studied by SEM. Details of sample preparation, prior publication of analyses, and the raw data are available from Wylie & Virta (2015b). Frequency of width is based on a bin interval of 0.110 μm. $N = 498$, N EMP = 439, N EMP >5 μm = 52.

CC. FERRO-ACTINOLITE, ONTARIO, CANADA, $PM_{2.5}$. The data are taken from Cyphert *et al.* (2012). They report that the sample was collected from the Marmora Mine, Marmora, Ontario, Canada. It was crushed and ground and subject to water elutriation to isolate respirable particles with aerodynamic diameters of less than 2.5 μm. Measurements were made by TEM. Frequency of width is based on a bin interval of 0.110 μm. $N = 420$, N EMP = 169, N EMP >5 μm = 5.

DD. Na-Ca AMPHIBOLE, MT. Amphibole particles extracted from treated and untreated vermiculate mined and treated by W.R. Grace and Company in Libby, Montana, were studied by TEM by the Ontario Research Foundation and Illinois Institute Technology Research Institute (IITRI) under EPA contract to Midwest Research Institute (MRI) (Atkinson *et al.* 1981). The chemical composition of the amphibole ranges over a number of amphibole nomenclature categories, but it is primarily winchite (80%) followed by richterite and tremolite (Meeker *et al.* 2003). It was called tremolite by Atkinson *et al.* (1981). Frequency of width is based on a bin interval of 0.125 μm. From untreated vermiculite [DD(a)]: N EMP = 427, N EMP >5 =151. From exfoliated vermiculite [DD(b)]: N EMP = 569, N EMP >5 μm = 236.

EE. AIRBORNE Na-Ca AMPHIBOLE, MT. Airborne particles identified as amphibole collected on air-monitoring filters from the town of Libby, Montana by Lee *et al.* (2009). Splits of the air filters were also analyzed by EPA (EPA 2006). The dust derives from gangue waste from the vermiculite mining present in many places in the town. Amphibole particles were measured by TEM. Frequency of width is based on a bin interval of 0.100 μm (data obtained from R.J. Lee, *pers. commun.*). N EMP >5 μm = 672.

FF. AIRBORNE Na-Ca AMPHIBOLE, MT. Airborne particles identified as amphibole were collected by the EPA on air-monitoring filters from the town of Libby, Montana. Splits of the air filters were also analyzed by Lee *et al.* (2009). Data were obtained from R.J. Lee (*pers. commun.*). The dust derives from gangue waste from mining vermiculite that is present in many places in the town. Amphibole particles were measured by TEM. Frequency of width is based on a bin interval of 0.110 μm. N EMP = 3208, N EMP >5 μm = 1740.

GG. Na-Ca AMPHIBOLE-ASBESTOS, MT. $PM_{2.5}$. Data are from amphibole from Cyphert *et al.* (2012). Amphibole asbestos from Libby, MT, was subject to water elutriation to isolate respirable particles with aerodynamic diameters of less than 2.5 μm. Measurements were made by TEM. Frequency of width is based on a bin width of 0.110 μm. $N = 645$, N EMP = 605, N EMP > 5 μm = 185.

HH. ANTHOPHYLLITE-ASBESTOS[3], Raw-NIST SRM. Asbestos purchased from Ward's Science from the Rakabedo Mines, near Udaipur, India, was characterized by RTI and sent to NIST to become a NIST SRM. The measurements were made by TEM from material retained by RTI. It was dispersed in water and selectively sampled for particles with L >5 μm and W <3 μm and AR >3:1 (Harper *et al.* 2008). RTI reports the presence of abundant talc which conforms to the NIST SRM data sheet. The data are from Beard *et al.* (2007) and were provided in electronic form by the National Institute of Occupational Safety and Health. Frequency of width is based on a bin interval of 0.121 μm. $N = 300$, N EMP = 274, N EMP >5 μm = 127.

TABLE 1. CONTINUED.

II. ANTHOPHYLLITE[1]. A nonfibrous mineral sample reported by Harper *et al.* (2008) to originate from Kopparberg, Sweden. The measurements were made by TEM from crushed and ground material. It was dispersed in water and selectively sampled for particles with L >5 μm, W <3 μm, and AR >3:1 (Harper *et al.* 2008). The data are taken from Beard *et al.* (2007) and were provided in electronic form by the National Institute of Occupational Safety and Health. Frequency of width is based on a bin interval of 0.120 μm. *N* = 300, *N* EMP = 155, *N* EMP >5 μm = 75.

[1] The electronic data sets received from NIOSH appear to have the labels of anthophyllite asbestos and common anthophyllite switched. This conclusion is based on (1) the NIST SRM anthophyllite asbestos description, which states talc is present 5–15%, a characteristic of the population mislabeled as anthophyllite cleavage population; (2) the RTI XRD pattern from Beard *et al.* (2007) for the sample mislabeled as anthophyllite asbestos that does not show talc; (3) the RTI analyst notes for the mislabeled anthophyllite asbestos that says the particles are blocky, more consistent with anthophyllite cleavage; and (4) the dimensional characteristics of the two populations.

TABLE 2. MEAN, MODAL, AND MEDIAN EMP WIDTHS (μm)

Shedd (1985) Crocidolite mines	Mean (geom.)	Mean (arith.)
Hamersley Range Western Australia	0.09	0.12
Hamersley Range Western Australia	0.08	0.09
NW Cape Province SA	0.06	0.07
NW Cape Province SA	0.09	0.11
Transvaal, SA	0.12	0.19
Transvaal SA	0.13	0.16
Transvaal SA	0.12	0.26
Transvaal SA	0.13	0.28
Bolivia	0.18	0.29

Churg & Wiggs (1986) Tremolite. Lung tissue. Occupational exposure to chrysotile. All lengths

	Mean (arith.)
shipyard	0.21
insulation	0.28
brake industry	0.24
textile industry	0.23
manufacturing	0.25
mining	0.21

Sebastien *et al.* (1989) Tremolite from lung tissue. Occupational exposure to chrysotile. L > 5 μm

	Mean (arith.)
Charleston SC textile	0.35
Thetford mining al milling	0.32

Paoletti & Bruni (2009) Tremolite from lung and pleura. Mesothelioma cases Basilicata, Italy L > 5μm

	Mean (geom.)	Mean (arith.)
pleura	0.34	0.33
pleura	0.33	0.32
lung	0.56	0.49
lung	0.55	0.46

TABLE 2. CONTINUED.

Timbrell (1982) Occupational exposure to anthophyllite. Finland. All lengths.

	median	modal
airborne mine	0.44	0.25
airborne mill	0.52	0.34
airborne bagging	0.7	0.36
lung tissue	0.57–0.76	0.36–0.78

Paoletti & Bruni (2009) Fluoro-edenite Biancaville, Italy. Mesothelioma cases L > 5μm

	Mean (geom.)	Mean (arith.)
pleura	0.31	0.34
pleura	0.30	0.32
lung	0.41	0.45
lung	0.42	0.47

Gibbs *et al.* (1991) Mesothelioma cases. Occupational exposure. All lengths. Geometric mean.

	amosite	crocidolite
subpleural parenchymal	0.17	0.1
central parenchymal	0.17	0.09
pleura	0.17	0.08

Warnock (1989) Mesothelioma cases. Occupational exposure. Tissue analysis. All lengths

	amosite	crocidolite	anthophylllite	actinolite	tremolite
median diameters	0.17	0.09	0.23	0.25	0.3

Dodson *et al.* (2004) Lung cancer and asbestosis cases. Tissue analysis. All lengths.

	amosite	crocidolite	anthophylllite	actinolite	tremolite
geometric mean	0.2	0.1	0.29	0.29	0.37
range	0.02–1.80	0.02–0.80	0.03–5.0	0.05–1.3	0.05–1.4

Gibbs *et al.* (1990) Mesothelioma cases. Paraoccupational exposure. Tissue analysis. All lengths

	amosite	crocidolite
Geometric mean	0.16–0.36	0.07–0.11

been found to be bimodal with two modes below 0.5 μm (Martha Warnock, *pers. commun.*).

While Australian crocidolite and Cape crocidolite likely produce dust clouds with similar dimensional characteristics, other occurrences of crocidolite are different. Shedd (1985) studied bulk samples of crocidolite from the Transvaal region of South Africa and from Bolivia and showed that these populations are characterized by larger average widths and smaller proportions with widths less than 0.1 μm than Cape or Australian crocidolite. Data are provided in Table 2.

Amosite

All amosite used worldwide comes from the Transvaal Asbestos Belt in South Africa. The frequency distributions of width and length of aerosolized amosite are shown in Figure 2 and width means, modes, and ranges for particular length segments are shown in Table 4. Airborne and lung-burden fibers of amosite are wider and their widths are more variable, both between samples and within samples, than Cape crocidolite. The proportion of "crocidolite-like" amosite fibrils (width ≈0.1 μm or less) and the range in width and length of airborne fibers from the mines and mills of South Africa are different from those from industrial locations in the United States (shipyard and electrical) where amosite was used (Table 4). Comparison of populations N and O suggests that the dimensional characteristics of airborne amosite fibers may also differ among mines or during mining. Even within industrial locations, applications in the shipyard produce amosite dusts

TABLE 3. CROCIDOLITE EMPS

	F(a) mine air	F(b) bagging air	D(a) mine air	D(b) Lung burden	E raw-NIST SRM	C NIEHS
$1 \leq L \leq 5$ μm						
% all EMPs	96	93	61*	64*	23	49
width mode (μm)	<0.06	0.15 ± 0.05	<0.125	<0.125	0.24 ± 0.06	0.22 ± 0.06
mean width ± SD (μm)					0.32 ± 0.15	0.24 ± 0.09
range (μm)			<0.125 to >0.375	<0.125–0.250	0.12–0.72	0.11–0.99
$5 < L \leq 10$ μm						
% all EMPs measured	3.1	6.2	13**	20**	47	25
width mode (μm)	0.15 ± 0.05	0.15 ± 0.05	0.125–0.250	<0.125	0.24 ± 0.06	0.22 ± 0.06
mean width ± SD (μm)					0.29 ± 0.18	0.26 ± 0.10
width range (μm)			<0.125 to >0.375	<0.125 to >0.375	0.12–0.84	0.11–1.1
$10 < L \leq 15$ μm						
% all EMPs measured	<1.0	<1.0	1***	3***	20	8
width mode (μm)	0.15 ± 0.05*	0.15 ± 0.05*	0.125–0.375	0.125–0.250	0.12 ± 0.06	0.22 ± 0.06
mean width ± SD (μm)					0.32 ± 0.19	0.28 ± 0.10
width range (μm)			<0.125 to >0.375	<0.125 to >0.375	0.12–0.96	0.11–0.75
$L > 15$ μm						
% all EMPs measured					9	16
width mode (μm)					0.24 ± 0.06	0.33 ± 0.06
mean width ± SD (μm)					0.50 ± 0.53	0.36 ± 0.19
width range (μm)					0.12–2.88	0.11–1.32
Number of EMPs					300	1030
maximum length (μm)	20	20			38	1485
minimum length (μm)					1.9	0.7

Note: * data for $1 \leq L \leq 4$ μm); ** data for $4 < L \leq 10$ μm; *** data for $L > 10$ μm.

TABLE 4. AMOSITE EMPS

	Aerosol						Bulk	
	L shipyard	M electrical	N(a) mine	N(b) lung	O(a) mine	O(b) bagging	K NIEHS	P raw-NIST SRM
$1 \leq L \leq 5$ μm								
% all EMPs	48	24	56*	57*	87.5	75.5	20	50
width mode (μm)	0.20 ± 0.05	0.20 ± 0.05	0.125–0.250	0.125–0.250	0.15 ± 0.05	0.15 ± 0.05	0.33 ± 0.06	0.36 ± 0.06
mean width ± SD (μm)	0.31 ± 0.22	0.31 ± 0.22					0.39 ± 0.19	0.63 ± 0.34
range (μm)	0.06–1.1	0.05–0.9	<0.125 to >0.375	<0.125 to >0.375			0.09–1.32	0.12–2.4
$5 < L \leq 10$ μm								
% all EMPs measured	32	32	24**	31**	10.5	17.0	18	35
width mode (μm)	0.35 ± 0.10	0.30 ± 0.05	>0.375	0.125–0.250	>0.30	>0.30	0.44 ± 0.06	0.72 ± 0.06
mean width ± SD (μm)	0.41 ± 0.24	0.40 ± 0.23					0.45 ± 0.24	0.71 ± 0.42
width range (μm)	0.10–1.3	0.05–1.0	<0.125 to >0.375	<0.125 to >0.375			0.11–1.76	0.24–2.4
$10 < L \leq 15$ μm								
% all EMPs measured	8	15	8***	9***	1.7***	6.3***	11	10
width mode (μm)	0.20 ± 0.05	0.30 ± 0.05	>0.375	>0.375	>0.30	0.3	0.44 ± 0.06	0.84 ± 0.06
mean width ± SD (μm)	0.47 ± 0.35	0.42 ± 0.29					0.51 ± 0.27	0.78 ± 0.42
width range (μm)	0.10–1.7	0.10–1.5	0.125 to >0.375	<0.125 to >0.375			0.11–1.76	0.24–2.4
$L > 15$ μm								
% all EMPs measured	11	29					50	4
width mode (μm)	0.30 ± 0.05	0.30 ± 0.05					0.44 ± 0.06	0.60 ± 0.06
mean width ± SD (μm)	0.55 ± 0.34	0.57 ± 0.33					0.62 ± 0.35	0.88 ± 0.54
width range (μm)	0.10–1.9	0.10–1.7					0.11–3.19	0.24–1.8
Number of EMPs	837	374					1015	292
maximum length (μm)	145	181			20	20	1848	31
minimum length (μm)	0.6	1.3					0.88	1.44

Note: * data for $1 \leq L \leq 4$ μm; ** data for $4 < L \leq 10$ μm; *** data for $L > 10$ μm.

TABLE 5. EMPS OF TREMOLITE–ACTINOLITE–FERRO-ACTINOLITE AND ANTHOPHYLLITE ASBESTOS

	Y tremolite Korea	X tremolite India	W ferro-actinolite South Africa	BB ferro-actinolite South Africa	AA actinolite raw-NIST SRM	Z tremolite raw-NIST SRM	HH anthophyllite India
$1 \leq L \leq 5$ μm							
% all EMPs	54.6	65.4	80.6	84.5	55.4	67.9	53
width mode (μm)	0.07 ± 0.02	0.22 ± 0.06	0.22 ± 0.06	0.22 ± 0.06	0.72 ± 0.06	0.48 ± 0.06	0.36 0.06
mean width ± SD (μm)	0.20 ± 0.19	0.36 ± 0.21	0.29 ± 0.11	0.30 ± 0.15	0.71 ± 0.25	0.68 ± 0.28	0.49 ± 0.28
range (μm)	0.03–1.56	0.08–1.18	0.11–0.73	0.12–0.99	0.2–1.56	0.12–1.44	0.06–1.23
$5 < L \leq 10$ μm							
% all EMPs	27.4	15.7	8.6	7.7	33	23.9	33
width mode (μm)	0.07 ± 0.02	0.33 ± 0.06	0.22 ± 0.06	0.22 ± 0.06	0.66 ± 0.12	1.48 ± 0.24	0.62 0.06
mean width ± SD (μm)	0.26 ± 0.33	0.71 ± 0.44	0.36 ± 0.18	0.45 ± 0.20	1.06 ± 0.48	1.48 ± 0.57	0.87 ± 0.52
range (μm)	0.03–4.76	0.18–1.79	0.13–1.06	0.17–0.87	0.48–2.16	0.6–3.12	0.06–2.46
$10 < L \leq 15$ μm							
% all EMPs	9.4	1.6	2.1	2.1	8.2	6.7	7
width mode (μm)	0.14 ± 0.05	undefined	0.55 ± 0.06	undefined	1.14 ± 0.06	undefined	0.62 0.06
mean width ± SD (μm)	0.39 ± 0.42	1.12 ± 0.64	0.45 ± 0.14	0.25 ± 0.18	1.28 ± 0.52	2.55 ± 0.64	1.51 ± 0.88
range (μm)	0.03–3.4	0.38–1.5	0.22–0.66	0.23–0.80	0.36–2.4	1.8–3.84	0.62–3.44
$L > 15$ μm							
% all EMPs	8.5	2.1	1	2.1	3	1.5	6
width mode (μm)	0.68 ± 0.05	undefined	undefined	undefined	undefined	undefined	3.69 0.06
mean width ± SD (μm)	0.49 ± 0.55	1.86 ± 1.72	0.49 ± 0.14	0.67± 0.78	1.07 ± 0.31	4.74 ±1.78	2.51 ± 1.19
range (μm)	0.06–3.4	0.1–4.22	0.4–0.73	0.27–2.7	0.72–1.56	3.48–6.0	0.86–4.92
Number of EMPs	1443	191	521	439	233	134	274
minimum length (μm)	1.02	0.45	0.33	0.57	1.44	1.2	0.74
maximum length (μm)	85	84	28	68	30	9	40

TABLE 6. Na-Ca AMPHIBOLE EMPS FROM LIBBY, MONTANA

	EE	FF	DD(a)	DD(b)	GG
$1 \leq L \leq 5$ μm					
% all EMPs	ND	45	57	55	60
width mode (μm)		0.25 ± 0.05	0.16 ± 0.07	0.16 ± 0.07	0.22 ± 0.06
mean width ± SD (μm)		0.35 ± 0.20	0.28 ± 0.23	0.27 ± 0.19	0.26 ± 0.17
range (μm)		0.03–1.5	0.06–1.56	0.06–1.19	0.07–1.1
$5 < L \leq 10$ μm					
% all EMPs measured	63	33	19	27	20
width mode (μm)	0.25 ± 0.05	0.25 ± 0.05	0.28 ± 0.06	0.28 ± 0.06	0.22 ± 0.06
mean width ± SD (μm)	0.57 ± 0.37	0.59 ± 0.40	0.51 ± 0.33	0.47 ± 0.28	0.34 ± 0.21
width range (μm)	0.07–2.5	0.08–2.5	0.06–1.88	0.06–1.88	0.1–1.15
$10 < L \leq 15$ μm					
% all EMPs measured	19	13	8	9	5
width mode (μm)	0.25 ± 0.05	0.25 ± 0.05	0.28 ± 0.06	0.28 ± 0.06	0.22 ± 0.06
mean width ± SD (μm)	0.84 ± 0.72	0.73 ± 0.56	0.49 ± 0.22	0.54 ± 0.30	0.46 ± 0.26
width range (μm)	0.1–4	0.1–3.0	0.19–1.0	0.13–1.56	0.2–1.1
$L > 15$ μm					
% all EMPs measured	16	8	8	6	6
width mode (μm)	0.95 ± 0.05	0.45 ± 0.05	0.28 ± 0.06	0.28 ± 0.06	0.33 ± 0.06
mean width ± SD (μm)	0.99 ± 0.79	1.01 ± 0.73	0.80 ± 0.53	0.84 ± 0.72	0.41 ± 0.18
width range (μm)	0.2–4.5	0.15–4.5	0.13–2.19	0.19–3.13	0.2–0.85
Number of EMPs	672	3208	427	568	605
maximum length (μm)	51	93	80	51	37
minimum length (μm)	5	0.5	0.4	0.4	0.4

with size characteristics that are different from dusts derived by amosite use for electrical applications. Geometric means and median width for amosite from other lung-burden studies given in Table 2 are consistent with the data shown in Figure 2: aerosolized and lung-burden amosite fibrils of about 0.2 μm in width are characteristic. The study by Cressey *et al.* (1982) that produced cross-sections of amosite fiber bundles showed fibrils of about this same width. The widths measured by Gibbs & Hwang (1980) (O) are slightly smaller, but may reflect the fibril size from that mine at the time the fibers were collected and do not appear representative of aerosolized amosite in general.

The frequency distribution of width and length from two bulk samples of amosite, raw-NIST SRM and NIEHS, are shown in Figure 3 and width mean, mode, and range for particular length segments are found in Table 4. As was the case for bulk crocidolite, the populations derived from bulk samples have larger modal widths and greater lengths than are found in aerosolized populations. They also differ from each other in several ways. Fewer fibers from the raw-NIST SRM sample have widths ≤ 0.33 μm and modal widths are larger. The modal width of short NIEHS amosite fibers is different from long fibers, but no such variation was observed in the raw-NIST SRM material. Given that the same laboratories employing different protocols produced like results from bulk samples of crocidolite, protocols and practices alone cannot account for these differences; it is likely that the NIEHS and raw-NIST SRM amosite samples contain fibers with different dimensional characteristics.

All samples of amosite (and Cape and Australian crocidolite) exhibit parallel extinction; there are no reported exceptions. Consistent with this observation and direct observation by electron microscopy, fibers greater than about 0.2 μm in size are either composed of multiple fibrils or are polysynthetically twinned with twin-plane spacing <0.2 μm.

Tremolite–actinolite–ferro-actinolite asbestos

Occurrences of tremolite–actinolite–ferro-actinolite asbestos are more widespread than amosite or crocidolite, and they are characterized by a large variability in fibril widths, both within and among occurrences. Bimodal width distributions are common. The frequency of width of two samples of commercially produced tremolite asbestos are shown in Figure 4a and of two samples of ferro-actinolite asbestos in Figure 4b; the frequencies of length are shown in

TABLE 7A. AIRBORNE AMPHIBOLE CLEAVAGE FRAGMENT EMPS

	U actinolite VA	J grunerite MN	G grunerite SD	V trem-act and hbd CA
$1 \leq L \leq 5$ μm				
% all EMPs	55	67	56	48
width mode (μm)	0.55 ± 0.06	0.55 ± 0.06	0.55 ± 0.06	0.3 ± 0.1
mean width ± SD (μm)	0.71 ± 0.32	0.70 ± 0.29	0.77 ± 0.29	0.59 ± 0.31
range (μm)	0.2–1.5	0.3–1.4	0.11–1.6	0.05–3.8
$5 < L \leq 10$ μm				
% all EMPs	30	27	35	34
width mode (μm)	1.16 ± 0.06	undefined	1.10 ± 0.06	0.7 ± 0.1
mean width ± SD (μm)	1.48 ± 0.80	1.59 ± 0.44	1.28 ± 0.54	1.29 ± 0.67
range (μm)	0.3–7.4	0.6–2.2	0.3–2.7	0.22–7.0
$10 < L \leq 15$ μm				
% all EMPs	9	2	7	11
width mode (μm)	undefined	undefined	undefined	2.5 ± 0.1
mean width ± SD (μm)	2.32 ± 0.93	2.05 ± 1.34	1.91 ± 0.76	2.17 ± 1.14
range (μm)	1–4.5	1.1–3.0	0.4–3.3	0.25–8.5
$L > 15$ μm				
% all EMPs	4	3	2	6
width mode (μm)	undefined	undefined	undefined	2.5 ± 0.1
mean width ± SD (μm)	3.77 ± 3.40	4.43 ± 1.15	1.68 ± 0.69	3.90 ± 3.39
range (μm)	0.8–1.2	3.3–5.6	0.9–2.9	0.4–30
Number of EMPs	427	86	361	3219
minimum length (μm)	0.8	1.2	1.2	0.6
maximum length (μm)	36	22	45	84

Figure 4c. Width means, modes, and ranges for specific length segments are given in Table 5. The Korean asbestos is dominated by extraordinarily narrow fibrils with prominent modal widths of 0.06 and 0.12 μm, characteristic of both long and short fibers, and among these four samples, Korean tremolite asbestos (Y) contains the highest proportion of long fibers. Indian tremolite asbestos (X) displays the greatest range in width and the highest proportion of the shortest fibers (<2 μm); its fibers are wider, and their width modes vary with length: 0.22 and 0.55 μm for short fibers and 0.33 and 0.77 μm for long fibers. Because the precision of the measurement of the Indian tremolite-asbestos was ±0.06 μm, a bimodal distribution of the narrowest fibers on the scale of the Korean sample, if present, would not have been resolved. In between these two extremes are the two ferro-actinolite asbestos samples: BB, a ferro-actinolite variety known as prieskaite, from Prieska, Northwest Cape Province, South Africa, where it occurs with crocidolite, and W, a variety known as mountain leather, also from South Africa. Like the Korean tremolite-asbestos, the range of width is small, the widths are bimodal, and modal widths are the same for long and short fibers. They differ from the Korean tremolite in that the modal widths are larger, but precision of the measurements for them also was ±0.06 μm. The major modal class for both long and short fibers is centered at 0.22 μm with a secondary mode centered between 0.44 and 0.55 μm.

Most fibers from the tremolite asbestos samples display parallel or near-parallel extinction, but fibers as wide 1 μm can be found that exhibit normal optical properties. These wide fibers are glassy and brittle; they are described as byssolite by Verkouteren & Wylie (2000). Byssolite fibers are particularly common in the Indian tremolite asbestos. The optical properties of both ferro-actinolite asbestos samples are anomalous, and neither contains particles from which normal optical properties can be measured.

Figure 5 shows the frequency distributions of width and length for two raw-NIST SRMs: tremolite asbestos and actinolite asbestos. The tremolite-asbestos (Z) was taken from an abandoned asbestos mine in California and the actinolite asbestos (AA) is from Virginia, where it was uncovered during building construction. These SRMs are considered to be asbestos because they are composed of parallel bundles of fibrils easily

TABLE 7B. AMPHIBOLE CLEAVAGE FRAGMENT EMPS DERIVED FROM CRUSHED SAMPLES

	Q tremolite NIEHS	R tremolite NIEHS	A riebeckite CA	B riebeckite CO	H grunerite SD	I grunerite Portugal	II anthophyllite Sweden	S tremolite CA	CC ferro-actinolite Ontario	T actinolite CA
$1 \leq L \leq 5$ μm										
% all EMPs	59	74	37	69	69	80	52	47	57	63
width mode (μm)	0.83 ± 0.17	0.18 ± 0.12	0.44 ± 0.06	0.63 ± 0.06	0.64 ± 0.07	0.36 ± 0.06	0.72 0.06	0.25 ± 0.06	0.25 ± 0.06	0.61 ± 0.06
mean width ± SD (μm)	0.77 ± 0.28	0.40 ± 0.29	0.63 ± 0.30	0.59 ± 0.31	0.59 ± 0.31	0.54 ± 0.31	0.71 ± 0.29	0.38 ± 0.23	0.36 ± 0.25	0.59 ± 0.33
range (μm)	0.33–1.76	0.06–1.45	0.17–1.76	0.06–1.27	0.01–1.27	0.06–1.45	0.24–1.44	0.08–1.2	0.09–1.4	0.06–1.51
$5 < L \leq 10$ μm										
% all EMPs	21	11	20	25	23	13	40	3	2	9
width mode (μm)	1.93 ± 0.17	undefined	0.66 ± 0.06	0.66 ± 0.06	0.89 ± 0.07	1.21 ± 0.06	1.80 0.12	undefined	undefined	1.21 ± 0.06
mean width ± SD (μm)	1.70 ± 0.49	1.14 ± 0.59	1.09 ± 0.56	1.56 ± 0.63	1.33 ± 0.62	1.30 ± 0.53	1.40 ± 0.50	0.90 ± 0.05	0.78 ± 0.33	1.45 ± 0.44
range (μm)	0.77–3.08	0.06–2.72	0.11–3.08	0.51–2.92	0.51–2.79	0.48–2.72	0.48–2.40	0.85–0.95	0.48–1.25	0.91–2.66
$10 < L \leq 15$ μm										
% all EMPs	10	5	9	4	2	3	5	0	0	2
width mode (μm)	3.3 ± 0.10	undefined	0.66 ± 0.06	undefined	undefined	undefined	undefined			undefined
mean width ± SD (μm)	2.76 ± 0.95	2.17 ± 0.94	1.66 ± 1.01	2.57 ± 1.01	2.88 ± 0.66	2.45 ± 1.03	2.76 ± 0.78			2.46 ± 1.38
range (μm)	0.99–4.4	0.48–3.33	0.33–3.96	1.52–4.44	2.22–3.81	0.97–3.93	1.44–3.60			0.61–4.24
$L > 15$ μm										
% all EMPs	11	2	33	2	1	< 1	4	0	0	<1
width mode (μm)	3.85 ± 0.08	undefined	0.77 ± 0.06	undefined	undefined	undefined	undefined			undefined
mean width ± SD (μm)	4.47 ± 3.10	3.95 ± 2.29	3.82 ± 3.30	3.77 ± 0.97	3.81 ± 2.29	undefined	2.70 ± 1.89			undefined
range (μm)	0.55–13.75	2.18–7.26	0.33–15.4	2.92–4.83	1.91–6.35	undefined	0.72–5.40			3.63
Number of EMPs	157	233	651	195	210	209	155	113	169	231
minimum length (μm)	1.1	0.6	0.44	0.64	0.8	0.5	1.2	0.26	0.36	0.33
maximum length (μm)	165	30	160	18.4	22	21	23.4	6	9	15.7

TABLE 8. FREQUENCY (%) OF EMP WIDTHS (W) IN SPECIFIED LENGTH SEGMENTS (L)

I. ASBESTOS

		L > 5 μm			L > 10 μm	L ≤ 5 μm		
1. Bulk Samples		W < 0.25 μm	W ≤ 0.33 μm	W ≤ 0.50 μm	W ≤ 0.33 μm	W < 0.25 μm	W ≤ 0.5 μm	Inst.
C	NIEHS crocidolite	46	83	95	71	67	98	SEM
E	Raw-NIST SRM Crocidolite	58	66	85	60	57	88	TEM
Y	Tremolite-asbestos Korea	55	65	82	52	76	93	TEM
BB	Prieskaite (ferro-actinolite)	16	49	72	28	42	95	SEM
W	Mountain leather (Ferro-actinolite)	13	38	62	25	49	88	SEM
K	NIEHS amosite	10	27	53	22	28	76	SEM
X	Tremolite-asbestos India	5	39	39	14	40	86	SEM
P	Raw-NIST SRM amosite	10	18	36	10	10	47	TEM
HH	Anthophyllite-asbestos India	8	10	20	0	27	61	TEM

		L > 4 μm		L > 10 μm	L < 4 μm	L < 4 μm	
2. Airborne and Lung Tissue		W < 0.250 μm	W < 0.375 μm	W < 0.375 μm	W < 0.25 μm	W < 0.375 μm	
D(a)	Crocidolite mine	72	89	75	93	98	TEM
D(b)	Crocidolite lung	82	96	87	97	>99	TEM
N(a)	Amosite mine	36	55	43	62	82	TEM
N(b)	Amosite lung	35	71	40	78	94	TEM

		L > 5μm			L > 10 μm	L ≤ 5 μm		
		W < 0.25 μm	W ≤ 0.33 μm	W ≤ 0.50 μm	W ≤ 0.33 μm	W < 0.25 μm	W ≤ 0.50 μm	
M	Amosite electrical (W)	22	45	68	39	50	87	SEM
L	Amosite shipyard (W)	26	46	69	42	50	88	SEM

		L > 5 μm			L ≤ 5 μm		
		W ≤ 0.2 μm	W ≤ 0.30 μm		W ≤ 0.20 μm	W ≤ 0.3 μm	
O(a)	Amosite mining	18	45	40	56	76	TEM
O(b)	Amosite bagging	15	32	25	41	65	TEM
F(a)	Crocidolite mining)	75	90	87	94	99	TEM
F(b)	Crocidolite milling	74	92	89	93	98	TEM

		L > 5 μm			L > 10 μm	L ≤ 5 μm		
3. Na-Ca amphibole, Libby MT		W < 0.25 μm	W ≤ 0.33 μm	W ≤ 0.50 μm	W ≤ 0.33 μm	W < 0.25 μm	W ≤ 0.50 μm	
FF	Town air	10	30	86	22	31	87	TEM
EE	Town air (RJL)	18	26	50	20	nd	nd	TEM
DD(a)	Extracted from raw vermiculite	8	21	55	29	54	89	TEM
DD(b)	Extracted from exfoliated product	12	34	60	27	48	92	TEM
GG	Selected for PM < 2.5	29	57	82	45	78	92	TEM

TABLE 8. CONTINUED.

		L > 5 μm			L > 10 μm	L ≤ 5 μm		
4. Raw-NIST SRM		W < 0.25μm	W ≤ 0.33 μm	W ≤ 0.50μm	W ≤ 0.33 μm	W < 0 .25 μm	W ≤ 0.50 μm	
Z	Raw-NIST SRM tremolite-asbestos	0	0	0	0	5	36	TEM
AA	Raw-NIST SRM actinolite-asbestos	0	<1	5	0	5	22	TEM

separable by hand pressure. However, they share little else in common with crocidolite, amosite, or the tremolite asbestos and ferro-actinolite asbestos occurrences shown in Figure 4. They lack fibrils greater than 5 μm in length that are also less than 0.2 μm in width. The width distributions are characterized by multiple modes, which are large in comparison to the other asbestos samples; the most well developed is 0.6–0.7 μm with a less prominent mode at about 0.9 μm (as discussed later, these modes are common in cleavage fragment populations). Only for short EMPs from the tremolite asbestos SRM is there a modal width class less than 0.5 μm; no widths less than 0.54 μm were found for long EMPs. The frequencies of length of the SRM populations are comparable to the Korean asbestos. The wider widths may contribute to the exclusion of short fibers because they do not attain an aspect ratio of 3. Parallel extinction is not characteristic of most fibers in these populations.

Tremolite asbestos that occurs with chrysotile has been identified as a likely cause of mesothelioma associated with exposure to chrysotile asbestos. Table 2 provides data from air and lung on the mean widths of the tremolite associated with the chrysotile deposits of Canada. Also given in Table 2 are mean widths of tremolite taken from pleural tissue of mesothelioma cases in Basilicata, Italy, where a cluster of mesothelioma cases occurs. Taking into account that the widths of the tremolite from Italy given in Table 2 are only for fibers >5 μm in length, their widths are similar to the tremolite associated with chrysotile exposure. The widths from Italian and Canadian chrysotile-associated tremolite are similar to the modal widths from tremolite and actinolite asbestos distributions shown in Figure 4; they do not resemble the raw-NIST SRMs in Figure 5. Little information is available for dimensions of the tremolite-asbestos implicated in mesothelioma among populations using tremolite-containing white wash (Constantopoulos 2008) with the exception that Langer *et al.* (1987) report that the widths and lengths of tremolite asbestos in whitewash from Metsovo, Greece, are statistically identical to

TABLE 8 (CONTINUED). FREQUENCY (%) OF EMP WIDTHS (W) IN SPECIFIED LENGTH SEGMENTS (L)

II. CLEAVAGE FRAGMENTS

		L > 5 μm			L > 10 μm	L ≤ 5 μm		
1. Bulk Samples		W < 0.25 μm	W ≤ 0.33 μm	W ≤ 0.50 μm	W ≤ 0.33 μm	W < 0.25 μm	W ≤ 0.50 μm	Inst.
I	Grunerite	0	0	3	0	21	61	TEM
H	Cummingtonite–grunerite	0	0	0	0	12	43	TEM
II	Anthophyllite	0	0	3	0	6	31	TEM
T	Actinolite	0	0	0	0	23	44	TEM
B	Riebeckite	0	0	0	0	13	38	TEM
A	Riebeckite	0.5	2	6	0	6	40	SEM
R	NIEHS tremolite	0	0	2	0	56	78	TEM
Q	NIEHS tremolite	0	0	0	0	0	16	SEM
S	Tremolite PM < 2.5	0	0	0	0	60	90	TEM
CC	Ferro-actinolite $PM_{2.5}$ < 2.5	0	0	trace	0	50	92	TEM
2. Airborne								
U	Actinolite	0	<1	3	0	0.4	36	SEM
G	Grunerite	0	0.6	9	0	0.5	26	SEM
J	Grunerite and actinolite	0	0	0	0	0	41	SEM
V	Tremolite, actinolite, hornblende	0	< 2	7	0	8	37	TEM

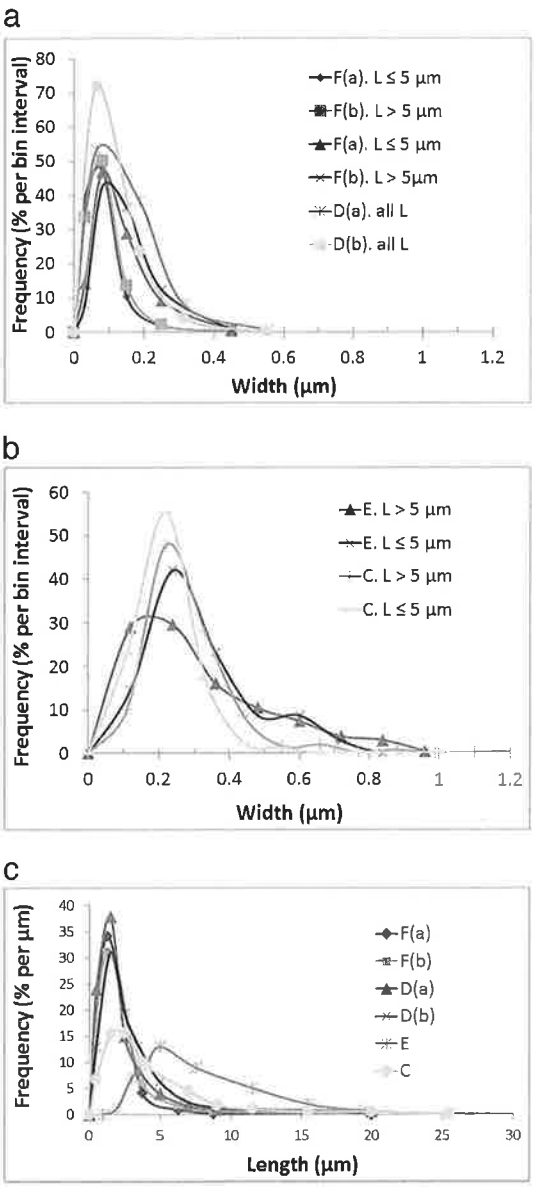

FIG. 1. Frequency of width and length of Cape crocidolite. (a) Frequency of width of aerosolized crocidolite. F(a) is from mine aerosol and F(b) is from the bagging area of the mill. D(a) is from the mine and D(b) is from the lung burden of miners who worked in the mine where D(a) was collected. Largest width class given for F (>0.300 μm) is plotted at 0.45 μm and the largest width class given for D (>0.375 μm) is plotted at 0.55 μm. (b). Frequency of width of bulk samples. E is raw-NIST SRM and C is NIEHS crocidolite. (c) Frequency of length. Approximately 6% of C is greater than 30 μm; maximum lengths are given in Table 2.

amosite and crocidolite measured under the same circumstances. In that case, they would be most similar to the tremolite asbestos from Korea. From my observations of this material, very thin EMPs displaying anomalous extinction angles are common, but byssolite is also present in the material, suggesting a greater similarity to the tremolite asbestos from India.

Anthophyllite asbestos

Figure 6 shows the frequency distributions for width and length, and Table 5 contains width means, modes, and ranges for specific length segments of anthophyllite asbestos from India. This asbestos contains many more wide EMPs than the other types of asbestos with the exception of the raw-NIST SRMs of tremolite and actinolite asbestos. The frequency distribution of width is multimodal, with modes centered at 0.12, 0.36, 0.61, and 0.97 μm, characteristic of both long and short fibers.

The major anthophyllite asbestos deposit in the world was located at Paakkila, Finland, and it has been extensively studied. Timbrell *et al.* (1970) published the width distribution of anthophyllite from the lung burden of occupationally exposed cases. It too shows a multimodal distribution of width with modes centered at about 0.35, 0.65, and 1 μm, very similar to the distributions shown in Figure 6. The width distribution of EMPs from bulk samples of the Union for International Cancer Control (UICC) anthophyllite asbestos from Paakkila also displays significant scatter and a multimodal distribution with six modes between 0.3 and 1.2 μm. Approximately 35% of the airborne fibers at Paakkila have widths less than 0.5 μm whereas 39% of the fibers shown in Figure 6 have widths less than 0.55 μm (Timbrell 1983). Timbrell (1982) reported the median width of airborne Paakkila anthophyllite asbestos as 0.44–0.70 μm (Table 2) while the median for the Indian anthophyllite asbestos is 0.67 μm. Modal widths for airborne Paakkila anthophyllite range from 0.25 to 0.36 μm (Table 2). These data point to the similarities between anthophyllite asbestos from India and Finland.

Watson (1999) examined samples of anthophyllite asbestos from many locations. He found that the smallest fibrils ranged in size from 0.05 to 0.4 μm and that prismatic lath-like anthophyllite particles from 0.3 to 4 μm in width were also present in the samples. Talc fibers were ubiquitous and ranged from <0.025 to 5 μm in width, presenting a complication in the dimensional analysis of anthophyllite asbestos. Fibrous talc does not seem to have the same pathogenic properties as amphibole (Wylie *et al.* 1997), yet it may be included in measurements because of its similarity in composition and size to anthophyllite asbestos.

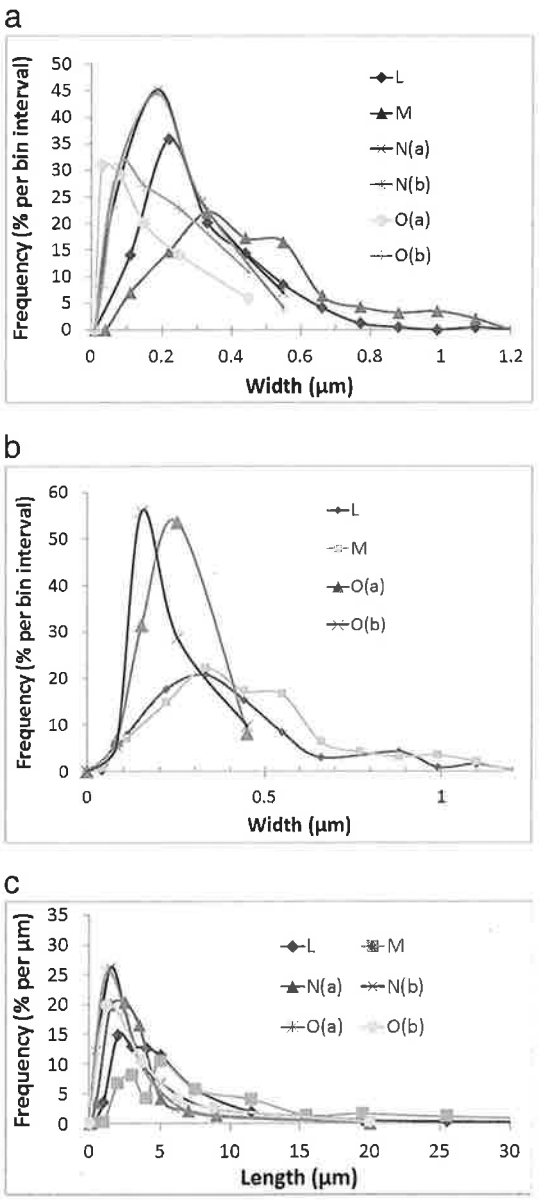

FIG. 2. Frequencies of width and length of aerosolized amosite. L and M are from air-monitoring filters collected in a shipyard and electrical company, respectively; N(a) is from mine aerosol and N(b) is from lung burden of miners who worked in the mine where N(a) was collected; O(a) is from mine aerosol and O(b) is from the bagging area of the mill. Maximum width interval for N is >0.375 μm; it is plotted at 0.55. Maximum width interval for O is >0.300 μm; it is plotted at 0.45 μm. (a) Frequency of width. Data from L, M, and O are for $L \leq 5$ μm. Data for O are for all lengths. (b) Frequency of width for $L > 5$ μm. Approximately 3% of populations L and M

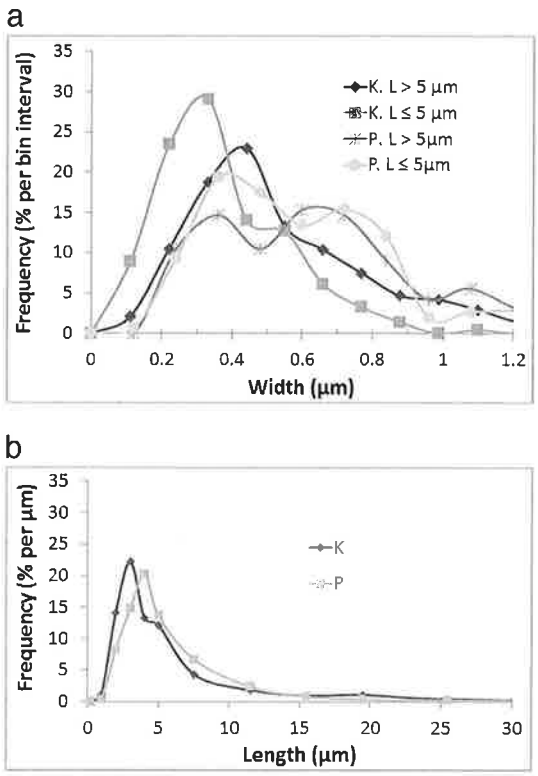

FIG. 3. Frequency of width and length of bulk samples of amosite. K is the NIEHS material and P is the raw-NIST SRM. (a) Frequency of width. One percent of population K ($L > 5$ μm), less than 5% of population P ($L \leq 5$ μm), and less than 10% of population P ($L > 5$ μm) are greater than 1.2 μm in width. Maximum widths are given in Table 4. (b) Frequency length. Less than 7% of K is greater than 30 μm in length.

Because anthophyllite is orthorhombic, parallel extinction is not diagnostic of a fibrillar structure. Careful measurement of indices of refraction should demonstrate only two indices of refraction if the EMPs are fibrillar and the fibrils are less than 0.2 μm in width. Three indices of refraction were measured for anthophyllite asbestos by Watson (1999), but from wider particles. Magnesium-rich anthophyllite asbestos is always intergrown with talc, resulting in lower indices of refraction and higher birefringence than

←

FIG. 2. (continued) have widths >1.2 μm; maximum widths are given in Table 4. (c) Frequency of length. Approximately 4% of population L and 9% of population M have lengths greater than 30 μm.

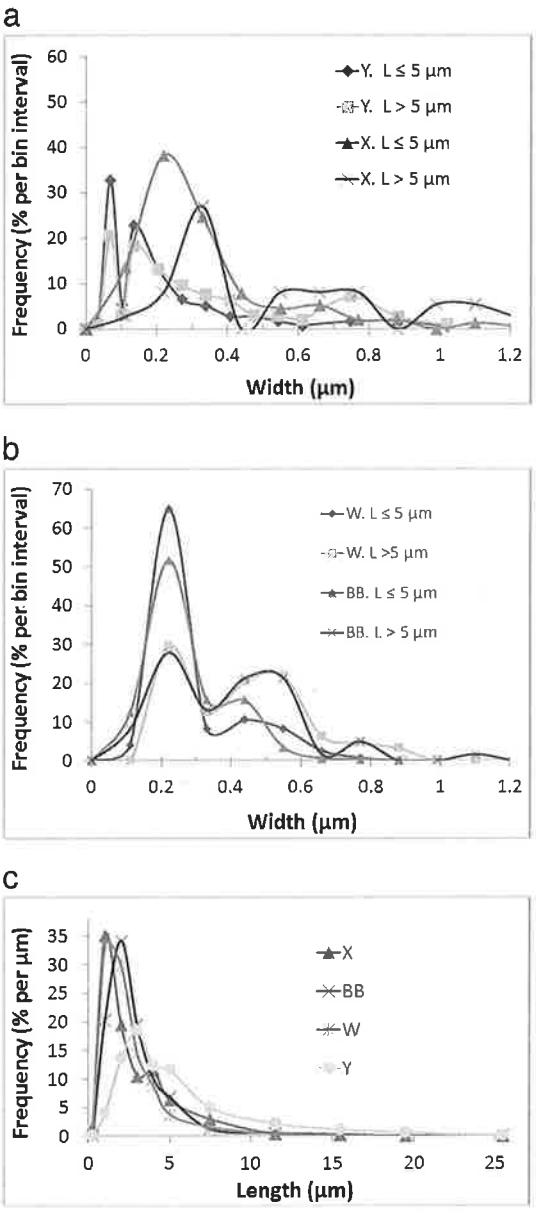

FIG. 4. Frequency of width and length of tremolite asbestos and ferro-actinolite asbestos. (a) Frequency of width derived from characterization of bulk samples of commercially mined tremolite asbestos from Korea (Y) and India (X). Approximately 15% of population X ($L > 5$ µm) is greater than 1.2 µm in width. Maximum widths are given in Table 5. (b) Frequency of width derived from bulk samples of actinolite asbestos, variety mountain leather (W), and ferro-actinolite asbestos, variety prieskite (BB). (c) Frequency of length of tremolite asbestos (X and Y) and ferro-actinolite asbestos (BB and W). Approximately 2% of populations Y and X are greater than 30 µm in length. Maximum lengths are given in Table 5.

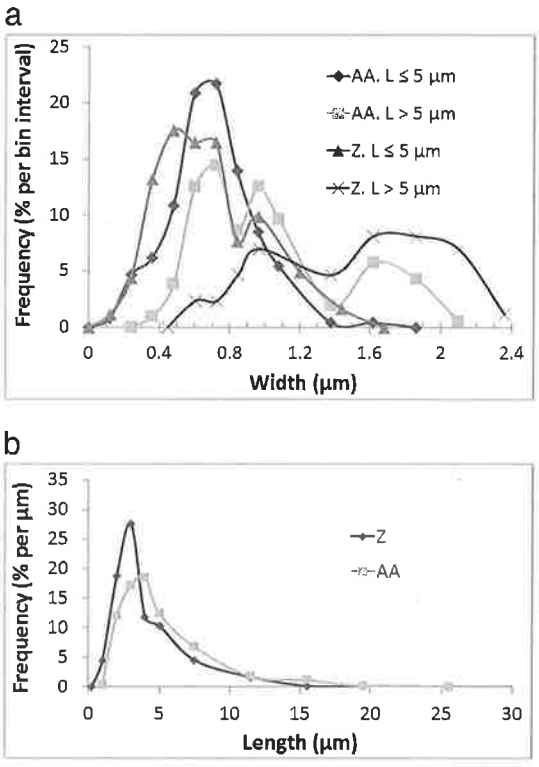

FIG. 5. Frequencies of length and width for raw-NIST SRMs of tremolite asbestos (Z) and actinolite asbestos (AA). (a) Frequencies of width. For Z ≈ 2% and ≈25% of short and long EMPs, respectively, are greater than 2.4 µm in width. Maximum widths are given in Table 5. (b) Frequency of length.

would be expected based on Mg/(Mg + Fe) alone (Watson 1999).

Na-Ca amphibole asbestos

The amphibole asbestos that occurs as gangue in the vermiculite deposit at Libby, Montana, is composed primarily of winchite, with lesser amounts of richterite, tremolite, and perhaps edenite (Meeker *et al.* 2003, Wylie & Verkouteren 2000). The deposit was prospected for asbestos, but the ore was of poor quality and the deposit has been mined only for vermiculite. The Na-Ca amphibole asbestos gangue was retained at the mine site and dispersed throughout the community as fill and road aggregate.

For convenience, the amphiboles from Libby will be referred to as Na-Ca amphibole. None of the characterizations consistently separate the amphiboles by composition, but all have used electron diffraction and chemical composition to identify the particles as

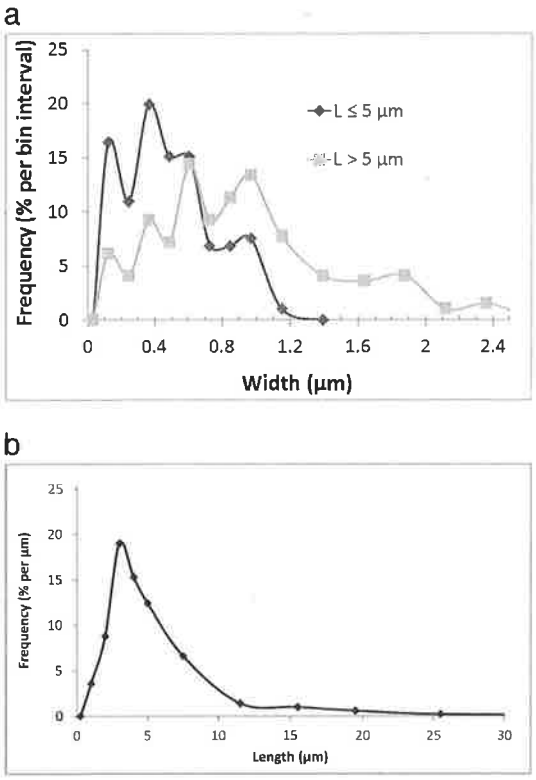

FIG. 6. Frequency of width and length of anthophyllite asbestos from India. (a) Frequency of width. Approximately 5% of EMPs longer than 5 µm are greater than 2.4 µm in width. Maximum widths are given in Table 5. (b) Frequency of length of anthophyllite asbestos. 2% of the EMPs are longer than 30 µm.

amphibole. The optical properties vary from the parallel extinction characteristic of asbestos to the more normal properties of most byssolite, so it is inhomogeneous in habit as well as composition. Despite the compositional and habit diversity found at Libby, the characterizations of width are remarkably similar.

Figure 7 shows the frequency distribution of width and length of EMPs isolated from vermiculite by elutriation; Table 6 provides width mean, mode, and range for specific length segments. The data (GG) from Cyphert *et al.* (2012) were derived by using water elutriation to produce particles from the gangue with aerodynamic diameter less than 2.5 µm to approximate respirable particles. Atkinson *et al.* (1981) measured fibers from elutriated samples of mine and mill products [DD(a)] and from exfoliated materials [DD(b)] with the intent of concentrating respirable particles. All three distributions show a dominant modal width of 0.1–0.2 µm for short fibers and a slightly larger modal width ≈0.3 µm for long fibers; the data from Atkinson *et al.* (1981) for mine and mill also contains a modal width ≈0.6 µm, not present in the exfoliated material. The frequencies of width appear to be unaffected by differences in the frequencies of length which are shown in Figure 7b.

The frequency distributions of width of EMPs recovered by elutriation are very similar to those shown in Figure 8a, which were derived from airborne EMPs collected in and around the town of Libby. The dominant modal width for short EMPs from the town aerosol is centered at about 0.25 µm with a secondary mode at about 0.55 µm, also characteristic of long EMPs. Long EMPs also show modal widths at approximately 0.75 and 1 µm. The similarities in mean and modal widths for the length segments given in Table 6 are noteworthy. The variance in width is largest for the EMPs collected on air monitoring filters in the town, perhaps reflecting more diversity in the habit of the amphiboles from that environment. The distribution of length is given in Figure 8b. Population FF contains a higher proportion of long EMPs than those collected from products. Only EMPs with length of 5 µm or greater were included in data set EE.

The asbestiform amphibole from Biancaville, Italy associated with an increased incidence of mesothelioma is fluoro-edenite. Paoletti & Bruni (2009) provide the dimensions of EMPs found in lung and pleural tissue of mesothelioma cases; mean widths for EMPs >5 µm can be found in Table 2. Their published distributions show that EMPs ≤0.2 µm in width, both longer and shorter than 5 µm, are present in lung and pleura burden. The high variance in widths moves mean values to 0.3–0.4 µm.

Airborne amphibole cleavage fragments

Measurements of length and width of amphibole collected on air monitoring filters are available from four locations. Figure 9a shows the frequency distribution of width from the Shadwell crushed stone quarry, Virginia (U), and from the Peter Mitchell taconite mine, Mesabi Range, Minnesota (J), both collected during mining. Figure 9b shows the frequency distribution of width from the Homestake Gold Mine, South Dakota (G), also collected during mining, and from El Dorado Hills, California (V), where air samples were taken during disturbance of the regolith. Figure 9c provides the length distributions from these four locations and Table 7a gives width means, modes, and ranges for specific length segments. Actinolite is the amphibole from the Virginia quarry, cummingtonite–grunerite and minor actinolite make up the EMPs from both the Minnesota and South Dakota mines, and

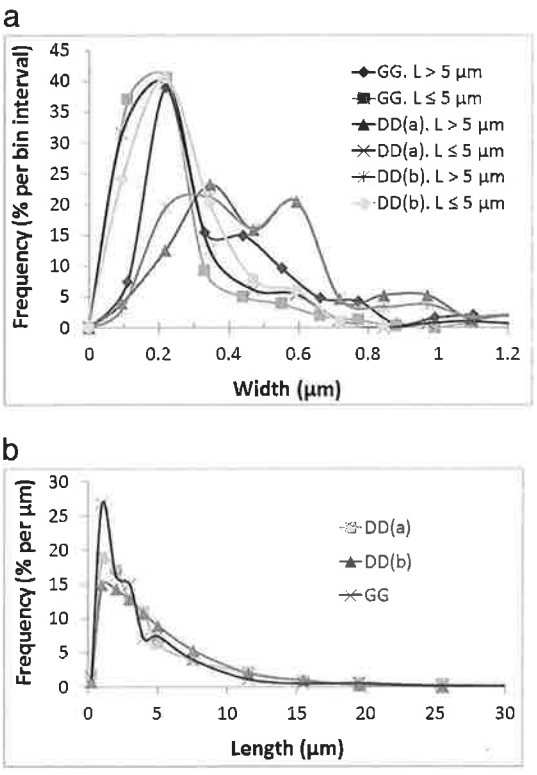

FIG. 7. Frequency of width and length of amphibole EMPs from Libby, MT selected for size by elutriation. GG was elutriated to $PM_{2.5}$. DD characterizations were derived from fibers removed from mine and mill vermiculite products (a) and from exfoliated vermiculite (b). (a) Frequency of width. Approximately 2% and 7% of EMPs shorter and longer than 5 μm, respectively, from population DD(a) and 6% of EMPs longer than 5 μm from population DD(b) are wider than 1.2 μm. Maximum widths are given in Table 6. (b) Frequency of length. Approximately 2% of EMPs from DD(a) and DD(b) are longer than 30 μm. Maximum lengths are given in Table 6.

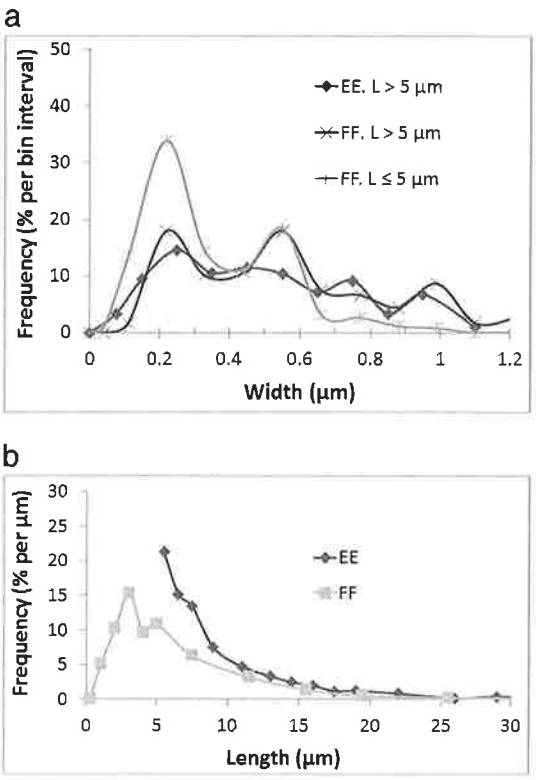

FIG. 8. Frequencies of length and width of airborne amphiboles collected on air monitoring filters in and around the town of Libby MT. Populations EE and FF were derived from analyses by two laboratories from splits of the same air filters; both were analyzed by TEM. (a) Frequency of width. 12% of EMPs in population EE and 10% of long fibers from population FF are greater than 1.2 μm in width. (b) Frequencies of length. Approximately 3% of EE and 2% of FF are longer than 30 μm.

the amphibole from El Dorado Hills contains Ca, Fe, and Mg (tremolite–actinolite) and Ca, Fe, Mg, and Al (hornblende and perhaps actinolite).

The width distributions are multimodal with the most prominent mode centered at about 0.6 μm for short EMPs and a less-pronounced mode at about 1.1 for long EMPs from Virginia, South Dakota, and California. The El Dorado amphibole also displays a smaller, more-prominent modal width at about 0.3–0.4 μm. For all length segments, the El Dorado amphiboles are narrower than the other three (Table 7a). Perhaps this difference reflects the dimensions of amphibole found in the regolith, where weathering has played a role in size and shape, while the source of the other three was crushed rock. The numbers of particles from the taconite mine is very small (only 37 > 5 μm in length), but more than 150 particles define each of the other curves and more than 3000 make up sample V from El Dorado. For all populations, the width of long EMPs is significantly larger than that of short (Table 7a).

Amphibole cleavage fragments from crushed samples

The complexities encountered in sampling and characterizing cleavage fragment populations from crushed samples are illustrated in Figures 10–13. Generally, samples of crushed amphibole contain EMPs with a wider range in width and length than is typical for airborne amphibole EMPs; selecting samples based

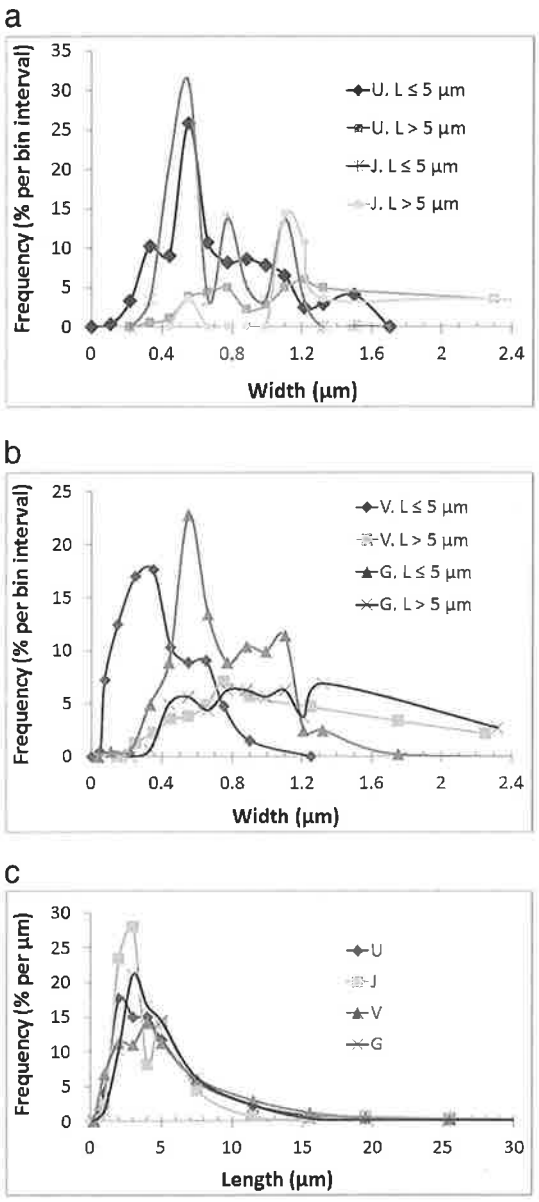

FIG. 9. Frequencies of width of airborne amphibole EMPs. U, J, and G were collected on air monitoring filters from mines. U is actinolite from an aggregate mine, VA, J is grunerite and actinolite from a taconite mine, MN, and G is from a gold mine in South Dakota. V was collected after disturbance of the regolith in El Dorado County, CA. (a) Frequency of width of U and J. Approximately 18% of EMPs in population U and 14% of population J that are longer than 5 µm are wider than 2.4 µm. Width ranges are given in Table 7a. (b) Frequency of width of V and G. Approximately 22% of EMPs longer than 5 µm in population V and 8% of population G are wider than 2.4 µm. Width ranges are given in Table 7a. (c) Frequency of length. Approximately 2% of EMPs in population G are greater than 30 µm in width. Length ranges are given in Table 7a.

on settling velocities restricts both length and width and impacts their distributions. Nonetheless, there are commonalities among the populations.

Shown in Figure 10 are the frequencies of width and length of the same material, NIEHS tremolite, sampled and characterized by two different laboratories following different protocols. Width means, modes, and ranges for specific length segments are shown in Table 7b. The relative abundances of particles ≤0.5 µm in width and less than 5 µm in length are not comparable. Particle sampling and measurement protocols for Q were designed to characterize the population as a whole by SEM (Campbell *et al.* 1980), while those for R were designed to represent the respirable fraction of the material by TEM (Harper *et al.* 2008). Nonetheless, both exhibit common characteristics: an abundance of particles less than 1 µm in width; longer EMPs that are wider than short ones; a lack of narrow, long EMPs; and a bimodal distribution of width, in this case modes centered at about 0.63 and 0.86 µm.

Figure 11 shows the frequencies of width and length derived from bulk samples of riebeckite from two locations; the materials were characterized by the same two laboratories following the same protocols used for the NIEHS tremolite. As was the case for NIEHS tremolite, selective sampling and TEM characterization (R) resulted in a population with a larger proportion of EMPs less than 0.5 µm in width and less than 5 µm in length. A characterization designed to represent the sample as a whole (A) resulted in a sample that contains many wider EMPs. As also was the case for NIEHS tremolite, both characterizations contain an abundance of particles less than 1 µm in width, longer EMPs that are wider than short ones, and rare narrow, long EMPs. For both, however, the increase in width with length is not as pronounced as it is for NIEHS tremolite (Table 7b). The orientation of the indicatrix in riebeckite cleavage fragments is consistent with well-developed parting on {100}, which increases the aspect ratio. Sample A is also unusual for cleavage-fragment populations because the width distribution is not multimodal, although a shoulder on the distribution suggests a poorly expressed secondary mode. Modal widths at 0.7–0.8 are found in long EMPS in both samples.

Figure 12 shows frequencies of length and width of three crushed amphiboles, cummingtonite–grunerite

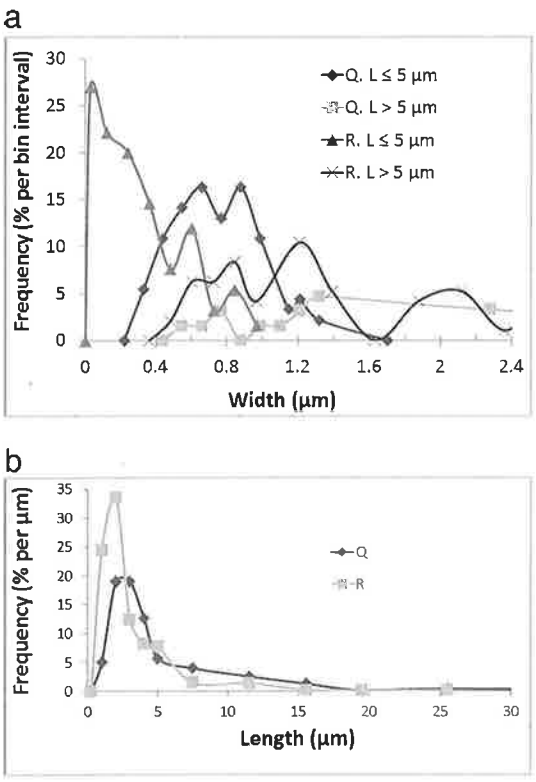

FIG. 10. Frequencies of width and length of NIEHS tremolite. The protocol followed for population Q was designed to characterize the sample as a whole; particles were measured by SEM. The protocol followed for population R included size selection by settling velocity in water to approximate respirable particles; measurement were by TEM. (a) Frequency of width. For EMPs longer than 5 µm, 21% of sample R and 35% of sample Q have widths greater than 2.4 µm (b) Frequency of length. 3% of population Q is greater than 30 um in length.

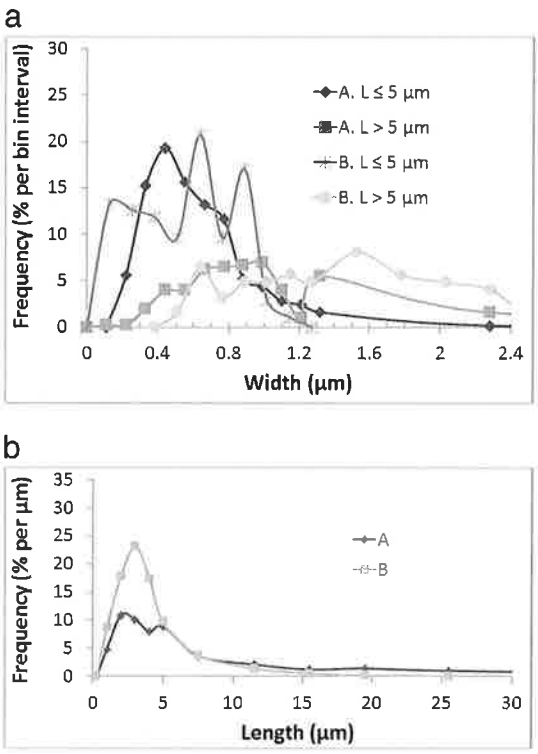

FIG. 11. Frequencies of width and length of two samples of crushed riebeckite. A is from California. The protocol measured EMPs by SEM. Sample B is from Colorado. Particles were selected by settling velocity to approximate respirable EMPS and measured by TEM. (a) Frequency of width. For EMPs longer than 5 µm, approximately 35% of population A and 22% of population B are wider than 2.4 µm. (b) Frequency of length. Approximately 16% of population A is longer than 30 µm.

from South Dakota [specific Mg/(Mg + Fe) not provided], grunerite from Portugal (I), and anthophyllite from Sweden (II). All were measured by TEM by the same laboratory following the same protocols. Data for width mean, mode, and range are given in Table 7b. The frequencies of width of all three are bimodal, but modes are slightly different; given that the same protocols were followed, it seems unlikely that counting bias is their source. Modes of 0.2–0.3 and 0.6–0.7 µm characterize short EMPs and 0.9 to 1.0 µm are prominent in long EMP populations, with the exception of the anthophyllite (II), for which a poorly expressed mode at 1.8 µm occurs for long EMPs.

Figure 13 shows frequencies of length and width of three samples of crushed amphibole in the tremolite–ferro-actinolite series which were size-selected by settling velocity. The techniques employed by Cyphert *et al.* (2012) (used also for Na-Ca amphibole from Libby) produced a population without EMPs longer than 10 µm and only a few between 5 and 10 µm. The modal widths of the short EMPs isolated by this technique are similar to those of asbestos, but the mean width of those few particles between 5 and 10 µm is much larger (0.9 and 0.8 µm Table 7b). The frequency of width of the crushed actinolite (T) shares characteristics in common with other samples of cleavage fragments. The populations are multimodal, with a well-developed mode at 0.61 µm for short EMPs and at 1.2 µm for long EMPs.

DISCUSSION

The frequency of both width and length provide insights into the nature of the growth habit of

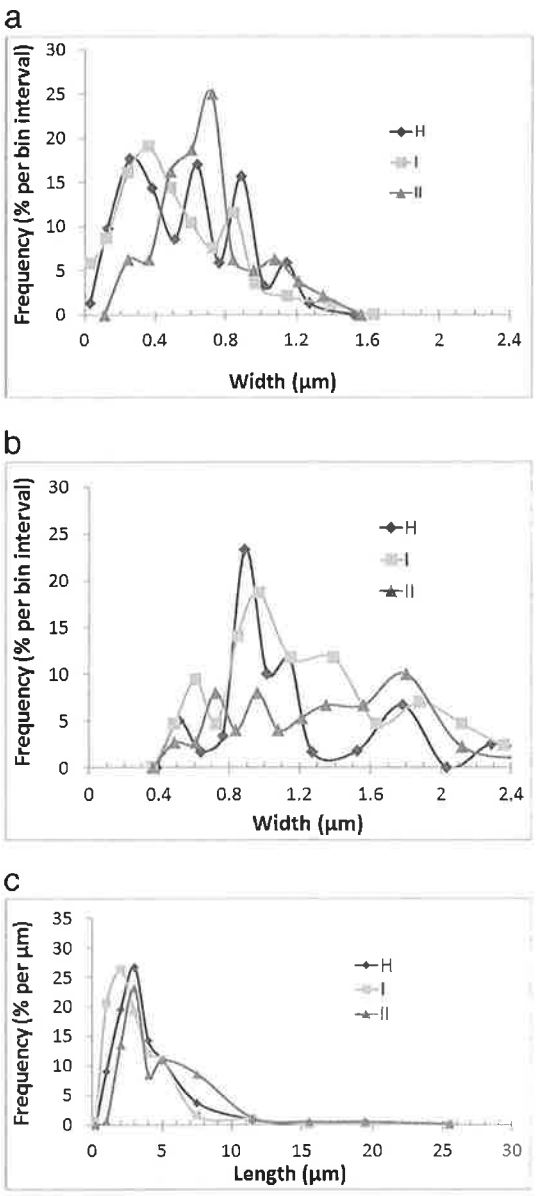

FIG. 12. Frequency of width and length of crushed cummingtonite–grunerite from Homestake Mine, SD (H), grunerite from Portugal, and anthophyllite from Sweden. Particles were selected by settling velocity to represent respirable EMPs. (a) Frequency of width of EMPs with L $\leq$ 5 μm. (b) Frequency of width of EMPs with L > 5 μm. Approximately 18%, 14%, and 7% of EMPS from H, I, and II respectively have widths greater than 2.4 μm. (c) Frequency of length.

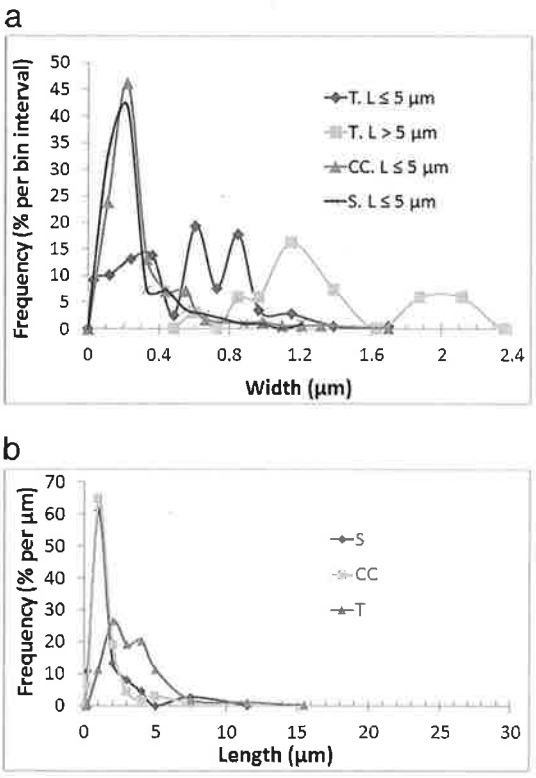

FIG. 13. Frequencies of width and length of EMPs derived from crushed amphibole. Population T is composed of particles of crushed actinolite from CA selected by settling velocity to represent respirable EMPs. CC and S were selected by elutriation to provide particles less than 2.5 μm in diameter. CC is ferro-actinolite from Canada, and S is tremolite from California. (a) Frequency of width. (b) Frequency of length.

amphibole asbestos. Fibril widths vary from <0.1 (Cape and Australian crocidolite and Korean tremolite) to as much as 0.7 μm (raw-NIST SRMs). Fibrils with the narrowest widths may be more than 100 μm in length. Many asbestos occurrences are characterized by width distributions that display several well-defined modes, *e.g.*, the two samples of ferro-actinolite asbestos from South Africa and Korean tremolite (Fig. 4), anthophyllite asbestos (Fig. 6), and the Na-Ca amphibole asbestos from Libby (Fig. 7). The reproducibility of multimodal distributions makes it unlikely that they are artifacts of counting protocols or sampling bias. Well-defined multiple modal widths probably reflect different periods of fibril formation. However, other factors, such as a regularly spaced alteration or secondary mineral growth between fiber bundles, cannot be ruled out for the larger modes, *e.g.*, talc associated with anthophyllite asbestos likely

influences bundle separation. In some cases, length distributions are bimodal, *e.g.*, those for tremolite-asbestos (Figs. 4 and 8). The high tensile strength of very thin fibrils keeps them from breaking, even when the samples are lightly ground; there is no such protection for wider fibrils, which are brittle. The presence of both types of fibrils may be signaled by a bimodality of length.

All asbestos is not the same. The length, width, and relative abundances of the smallest fibrils from deposits of different kinds of asbestos are different. Asbestiform varieties of the same mineral cannot be assumed to have fibrils of the same size, as the data from Shedd (1985) demonstrate for crocidolite (Table 2). An even wider variation in fibril size occurs among asbestos in the tremolite–actinolite–ferro-actinolite series (Table 5). Aerosol characteristics of amosite EMPs vary between mines and between mining and industrial applications (Table 4, Fig. 2). In biological experimentation, if dose is measured by weight, the number of fibers can be expected to vary significantly among samples.

As Stanton *et al.* (1981) pointed out, correlations with carcinogenic potential may be significant for a number of dimensional parameters, because they correlate with each other. Furthermore, exposure is to a population of particles. For this reason, determining which fibers in an asbestos population are most carcinogenic remains somewhat uncertain. It would be useful if there were a proxy for potency that could be applied to a population as a whole. There are a number of parameters that could be used to predict potency for mesothelioma based on equivalent doses of EMPs of a particular length. For example, by applying the suggestions by Lippmann (2014) and Timbrell (1983) that fibers longer than 5 μm must be ≈0.1 μm (or less) in width to cause mesothelioma, if there were equivalent doses of EMPs longer than 5 μm, the mesothelioma incidence might be expected to follow the frequencies of fibrils ≤0.1 μm in width within the set of EMPs >5 μm. For some of the populations in this study, the smallest widths recorded were 0.22 μm, but for those that include width measurements ≈0.1 μm, the frequencies are: 2–8% for Libby Na-Ca amphibole, 6% for anthophyllite asbestos, 10–15% for amosite, 56% for Korean tremolite asbestos, and 10–90% for crocidolite (bulk *versus* aerosolized).

Other proxies that might be used to predict potency are the proportion of fibers longer than 5 μm that are less than ≤0.33 μm (or <0.25 μm) in width or the proportion of fibers longer than 10 μm that are ≤0.33 μm in width. These are given in Table 8. Particles longer than 5 μm and ≤0.3–0.4 μm in width have been shown to be retained by the lung and preferentially transported to the pleura (unless otherwise specified, in this study, the width parameters are bin midpoints, so widths designated as ≤0.33 μm have an uncertainty of about ±0.06 μm, and the 0.33 μm bin includes widths 0.27–0.39 μm). It has also been proposed that the most mesotheliomagenic fibers are very thin fibers >10 μm in length.

Using the frequency of width ≤0.33 μm among EMPS longer than 5 μm as a proxy for potency yields 10% for anthophyllite asbestos, 18–27% for amosite, 21–34% for Na-Ca amphibole at Libby (excluding GG), 65% for Korean tremolite, 49–65% for ferro-actinolite asbestos, and 66–83% for Cape "crocidolite". The fluoro-edenite asbestos from Biancavilla, Italy, implicated in mesothelioma contains long fibers with widths ≤0.33 μm, but their abundances are unknown. The percentage of EMPs longer than 10 μm that have width ≤0.33 μm as a proxy for potency yields 0% anthophyllite, 22–28% Na-Ca amphibole from Libby MT, 22–43% amosite, 52% for tremolite asbestos from Korea, and 60–89% crocidolite. This proxy implies no risk from anthophyllite asbestos. None of the proxies imply risk from either the raw-NIST SRM tremolite asbestos or the raw-NIST actinolite asbestos (assuming the characterizations represent the aerosol) because they lack EMPs with the appropriate dimensions. Biological experimentation with the NIST SRMs would likely be informative.

Cleavage fragments lack narrow, long EMPs. Only riebeckite from California and grunerite from the aerosol at the Homestake Mine contain any long EMPs with widths ≤0.33 μm (2 and 0.6% respectively) and none are longer than 10 μm. Applying the proxies for EMP potency for mesothelioma described for asbestos yields potencies for mesothelioma that are either very small or zero.

In addition to assessing mesothelioma potential from metrological measures in the aerosol or bulk sample, the propensity of fibers to disaggregate into component fibrils after inhalation may be an important parameter in determining effective dose and mesothelioma risk. Cook *et al.* (1982) found limited disaggregation of fibrils of amosite in rats after intratracheal installation, but under the same protocols, they demonstrated significant disaggregation of ferro-actinolite asbestos. They attribute the higher disease outcome from ferro-actinolite to disaggregation of fibrils and an increase in effective dose after inhalation. Sheet silicates, hydroxides, magnetite, and other silicates may be intergrown with some amphibole asbestos (*e.g.*, Gunter *et al.* 2008, Veblen & Burnham 1977, Veblen 1980, Vermaas 1952, Ahn & Busek 1991, Watson 1999). Cressey *et al.* (1982) observed semi-coherent structural elements connecting independent amosite fibrils. When present, intergrowths or structural congruence will change the properties of derived dusts, both chemically and physically, when compared to amphibole-only fibrils

by increasing fiber widths, limiting disaggregation, and altering the fiber surface. A tail extending from the major mode toward higher magnitudes in the frequency distribution of width is indicative of fibril bundles and may indicate resistance to disaggregation. This tail is absent or only slightly developed in crocidolite populations (Fig. 1), but it is characteristic of long amosite fibers (Figs. 2 and 3). Interestingly, it is absent in the two ferro-actinolite asbestos samples shown in Figure 4 which occur with crocidolite in the Cape asbestos field. Asbestos mines produce different grades of material for different applications, usually by air classification, which in general differ in the proportion of long fibers. Longer fibers may resist disaggregation more effectively, as observed in larger widths of the amosite aerosols from industrial sources (Fig. 3). Disturbance of asbestos *in situ* may contribute to disaggregation of fibrils in different ways, strongly influencing the characteristics of dust clouds. Because parameters based only on frequency of thin fibers do not readily explain a 5–10-fold higher potency for crocidolite over amosite, perhaps it is crocidolite's tendency to readily disaggregate once inhaled that increases the effective dose well beyond what an exposure assessment might predict.

The data from the asbestos populations analyzed in this study were gathered with varying precision and covered varying ranges in length. Those with precision on the order of ± 0.06 μm may not provide the detail necessary to evaluate the presence of populations of very thin fibrils, such as have been measured under high magnification TEM in Korean tremolite asbestos (X) and the crocidolite characterized by Shedd (1985). Since it is known that cells respond in unique ways to particles on the order of 0.1 to 0.3 μm, and because disease induction appears to be related to fibers with small widths, high-precision measurements by TEM should be made to better understand the abundances of very fine fibrils of samples that will be used in cell or animal experimentation; this is particularly important when dose is administered by weight, but response is evaluated by fiber number. It is also important in assessing risk to humans. The use of TEM, however, presents challenges to describing the length distributions fully. The high magnifications necessary for width measurements may not be as useful for measuring the longest fibers, *e.g.*, compare E measured by SEM to C measured by TEM in Figure 2, and the range in length of K measured by SEM to P measured by TEM in Table 2. None of the populations described in this paper used the techniques of stratified sampling, which may be useful in overcoming this problem.

While asbestos fibrils attain their size and shape during crystallization, amphibole cleavage fragments attain their size and shape by crushing (or in some cases, weathering). The width characteristic of a particular length reflects not only the perfection of the cleavage (which likely varies somewhat among amphibole compositions) but also the development of parting (parallel to the **c**-axis in amphiboles is common) and the presence of intergrowths and alteration. These structural weaknesses affect aspect ratio, frequency of width, and the frequency of length. Despite these variables, the cleavage fragment EMP populations studied are remarkably similar. They contain an abundance of particles less than 1 μm in width, both their width and aspect ratio increase with length, and multimodal distributions of length and width are characteristic. A modal width of about 0.6 μm is common. Its origin is unknown, but perhaps a combination of the 3:1 aspect ratio requirement for an EMP and sampling techniques preferentially favor this width. There is also a common modal width centered at 0.2–0.3 μm among samples selected for particle size by elutriation and in aerosol from El Dorado Hills, California, but it is restricted to particles ≤ 5 μm in length.

A comparison of the frequency of width of sample G (Fig. 9) derived from air monitoring filters at Homestake Mine, South Dakota, to the frequency of width of sample H, crushed cummingtonite–grunerite, also from the Homestake Mine, shows that metrological characteristics of a sample crushed in a laboratory are expressed in the aerosol. Both populations have modal widths centered at $\approx$0.6, 0.9, and 1.1 μm. These data support the argument that the cleavage and partings that determine width are inherent to the material and are expressed in cleavage fragments of both bulk and airborne EMPs. Similar conclusions on the factors that control shape were drawn by Wylie & Schweitzer (1982) in their study of wollastonite. Sampling protocols may introduce differences, *e.g.*, the sampling protocol followed for the lab sample from Homestake produced a prominent width mode at about 0.2 μm, which is found only as a small shoulder on the major mode of the mine aerosol.

The tremolite and ferro-actinolite cleavage fragment EMPs elutriated to obtain respirable particles by Cyphert *et al.* (2012) are composed almost entirely of short, very fine particles with modal width of 0.2 μm. Only a few particles longer than 5 μm were included in their data sets. They used the same techniques to obtain the distribution of the Na-Ca amphibole asbestos from Libby shown in Figure 5a (GG), for which 31% were longer than 5 μm, so it was not the technique that precluded the inclusion of long thin particles, but rather their absence in the starting material. The argument that cleavage fragments with sizes that are characteristic of asbestos would be equally mesotheliomagenic cannot be tested by any of the populations described in this paper because they are absent.

Medians and modes are frequently used to describe and compare mineral fiber populations. However, the distributions of width and length are not normal and should not be assumed to be log normal, either. This fact limits the utility of using means to characterize and compare populations in terms of width and length and favors the use of ranges and modes.

In the United States the membrane-filter method is used to assess asbestos exposure in occupational settings, including mining (Leidel *et al.* 1979). In the absence of evidence to the contrary, the method requires that any optically visible EMP of tremolite–actinolite–ferro-actinolite, anthophyllite, riebeckite, or cummingtonite–grunerite longer than 5 μm be considered an asbestos fiber. Those TEM methods designed to provide equivalence to the membrane-filter method exclude EMPs less than 0.25 μm in width. Amphibole is common in many mines and quarries, making this a serious problem for the mining industry. Table 8 summarizes data from all populations examined in this study. The percentages of particles $>$ and $\leq$ to 5 μm in length that are <0.25 underscores this problem. Almost all EMP amphibole cleavage fragments in an aerosol can be expected to be >0.25 μm in width and counted in an exposure assessment, while large portions of asbestos fiber populations are less than 0.25 μm in width and are excluded. It is impossible to compare one asbestos exposure to another or to compare asbestos to cleavage fragment exposures or to predict the relative risk for mesothelioma by a continued reliance on optical microscopy (or TEM equivalents) for quantitative measurements of exposure. Developing an exposure assessment that uses TEM and is based on the abundance of long, narrow fibers would address this problem.

Acknowledgments

Thanks to the Bureau of Mines for research support to the University of Maryland that resulted in the collection of many of the data sets, and to the Library of the University of Maryland for housing them. Thanks also to Frank Hearl, Rich Lee, and Jenny Verkouteren for making data sets available, to Cyphert *et al.* (2012) for publishing theirs, and to my former students, collaborators, and others who took great care in the collection of dimensional data and thereby made this work possible. The paper benefitted significantly from the comments of two anonymous reviewers.

References

Addison, J. & McConnell, E.E. (2008) A review of carcinogenicity studies of asbestos and non-asbestos tremolite and other amphiboles. *Regulatory Toxicology and Pharmacology* **52**, S187–199.

Ahn, J.H. & Busek, P.R. (1991) Microstructures and fiber-formation mechanisms of crocidolite asbestos. *American Mineralogist* **76**, 1467–1478.

Amandus, H., Wheeler, R., Jankovic, J., & Tucker, J. (1987) The morbidity and mortality of vermiculite minerals and millers exposed to tremolite-actinolite part 1–2: Exposure estimates. *American Journal of Industrial Medicine* **11**, 1–14.

Atkinson, G.R., Rose, D., Thomas, K., Jones, D., Chatfield, E., & Going, J. (1981) Collection, analysis and characterization of vermiculite samples for fiber content and asbestos contamination. Midwest Research Institute report for the US Environmental Protection Agency Project 4901-A32 under EPA Contract 68-01-5915, Washington D.C., United States.

Aust, A.E., Cook, P.M., & Dodson, R.F. (2011) Morphological and chemical mechanisms of elongated mineral particle toxicities. *Journal of Toxicology and Environmental Health B* **14**, 40–75.

Beard, M.E., Ennis, J.T., Crankshaw, O.S., Doorm, S.S., Greene, L.C., Winstead, W.W., & Harvey, B.W. (2007) *Preparation of Non-asbestiform Amphibole Minerals for Method Evaluation and Health Studies Summary Report and appendices*. Prepared for Martin, Harper, NIOSH, Morgantown, WV by RTI International (Personal communication Frank Hearl CDC/NIOSH/OD).

Berman, D.W. & Crump, K.S. (2003) Final draft: Technical support document for a protocol to assess asbestos-related risk. United States EPA, Washington D.C., EPA #9345.4-06.

Berman, D.W. & Crump, K.S. (2008) A meta-analysis of asbestos-related cancer risk that addresses fibers size and mineral type. *Critical Reviews in Toxicology* **38**, 49–73.

Campbell, W.J., Steel, E.B., Virta, R.L., & Eisner, M.H. (1979) *Relationship of Mineral Habit to Size Characteristics for Tremolite Cleavage Fragments and Fibers*. Bureau of Mines Report of Investigations 8367. US Department of the Interior.

Campbell, W.J., Huggins, C.W., & Wylie, A.G. (1980) Chemical and physical characterization of amosite, chrysotile, crocidolite and nonfibrous tremolite for oral ingestion studies by the National Institute of Environmental Health Sciences. United States Bureau of Mines Report of Investigation **8452**.

Carbone, M., Ly, B.H., Dodson, R.F., Pagano, I., Morris, P.T., Dogan, U.A., Gazdar, A.F., Pass, H.I., & Yang, H. (2012) Malignant mesothelioma: Facts, myths and hypotheses. *Journal of Cell Physiology* **227**, 44–58.

Case, B.W., Abraham, J.L., Meeker, G., Pooley, F.D., & Pinderton, K.E. (2011) Applying definitions of "Asbestos" to environmental and "Low dose exposure levels and health effects, particularly malignant mesothelioma. *Journal of Toxicology and Environmental Health Part B* **14**, 3–39.

Churg, A. & Wiggs, B. (1986) Fiber size and number in workers exposed to processed chrysotile asbestos, chrys-

otile miners, and the general population. *American Journal of Industrial Medicine* **9**, 143–152.

Constantopoulos, S.H. (2008) Environmental mesothelioma associated with tremolite asbestos: Lessons from the experiences of Turkey, Greece, Corsica, New Caledonia and Cyprus. *Regulatory Toxicology and Pharmacology* **52**, S110–S115.

Cook, P.M., Palekar, L.D., & Coffin, D.L. (1982) Interpretation of the carcinogenicity of amosite asbestos and ferroactinolite on the basis of retained fiber dose and characteristics in vivo. *Toxicology Letters* **13**, 151–158.

Cressey, B.A., Whittaker, E.J.W., & Hutchison, J.L. (1982) Morphological and alteration of asbestiform grunerite and anthophyllite. *Mineralogical Magazine* **46**, 77–87.

Cyphert, J.M., Nyska, A., Mahoney, R.K., Schladweiler, M.C., Kodavanti, U.P., & Gavett, S.H. (2012) Sumas Mountain chrysotile induces greater lung fibrosis in Fischer 344 rats than Libby amphibole, El Dorado tremolite and Ontario ferroactinolite. *Toxicological Sciences* **130**, 405–425.

Dodson, R.F., Atkinson, M.A.L., & Levin, J.L. (2003) Asbestos fiber length as related to potential pathogenicity: A critical review. *American Journal of Industrial Medicine* **44**, 291–297.

Dodson, R.F., Brooks, D.R., O'Sullivan, M., & Hammar, S.P. (2004) Quantitative analysis of asbestos burden in a series of individuals with lung cancer and a history of exposure to asbestos. *Inhalation Toxicology* **16**, 637–647.

Dorling, M. & Zussman, J. (1987) Characteristics of asbestiform and non-asbestiform calcic amphiboles. *Lithos* **20**, 469–489.

Driscoll, M.K., Sun, X., Guven, C., Fourkas, J.T., & Losert, W. (2014) Cellular contact guidance through dynamic sensing of nanotopography. *ACS Nano* **8**, 3546–3555.

Ecology & Environment Incorporated (EEI) (2005) *El Dorado Hills naturally occurring asbestos multimedia exposure assessment El Dorado Hills*. California Preliminary Assessment and Site Inspection Report Interim Final, LabCor Contract No. 68-W-01-012; TDD No.: 09-04-01-0011; Job No.: 001275.0440.01CP. (R.J. Lee, personal communication).

EPA U.S. (2006) U.S. Environmental Protection Agency Produced Access Database, Libby Montana Airborne particles. *In* The matter of United States of America (W.R. Grace, ed.). CR-05-070M-DWM (D. Montana), 2005-2006.; (R.J. Lee, personal communication).

Gamble, J.F. & Gibbs, G.W. (2008) An evaluation of the risks of lung cancer and mesothelioma from exposure to amphibole cleavage fragments. *Regulatory Toxicology and Pharmacology* **52**, S154–S186.

Gibbs, G.W. & Hwang, C.Y. (1980) Dimensions of airborne asbestos fibers. *In* Biological Effects of Mineral Fibers **1** (J.C. Wagner, ed.). IARC Scientific Publication #30 Lyon, France (69–77).

Gibbs, A.R., Griffiths, D.M., Pooley, F.D., & Jones, J.S.P. (1990) Comparison of fibre types and size distributions in lung tissues of paraoccupational and occupational cases of malignant mesothelioma. *British Journal of Industrial Medicine* **47**, 621–626.

Gibbs, A.R., Stephens, M., Griffiths, D.M., Blight, B.J.M., & Pooley, F.D. (1991) Fibre distribution in the lungs and pleura of subjects with asbestos related diffuse pleural fibrosis. *British Journal of Industrial Medicine* **48**, 762–770.

Gunter, M.E., Harris, K.E., Bunker, K.L., Wyss, R.K., & Lee, R.J. (2008) Amphiboles between the sheets: observations of interesting morphologies by TEM and FESEM. *European Journal of Mineralogy* **20**, 1035–1041.

Harper, M., Lee, E.G., Dorn, S.S., & Hammond, O. (2008) Differentiating non-asbestiform amphibole and amphibole asbestos by size characteristics. *Journal of Occupational and Environmental Hygiene* **5**, 761–770.

Hochella, M.F. (1993) Surface chemistry, structure and reactivity of hazardous mineral dust. *In* Health Effects of Mineral Dusts (G.D. Guthrie & B.T. Mossman, eds.). Mineralogical Society of America Washington D.C., *Reviews in Mineralogy* **28**, 275–302.

Hodgson, J.T. & Darnton, A. (2000) The quantitative risks of mesothelioma and lung cancer in relation to asbestos exposure. *Annals of Occupational Hygiene* **44**, 565–601.

Huang, S.X.L., Jaurand, M.C., Kamp, D.W., Whysner, J., & Hei, T.K. (2011) Role of mutagenicity in asbestos fiber-induces carcinogenicity and other diseases. *Journal of Toxicology and Environmental Health B* **14**, 179–245.

Hume, L.A. & Rimstidt, J.D. (1992) The biodurability of chrysotile asbestos. *American Mineralogist* **77**, 1125–1128.

Langer, A.M., Nolan, R.P., Constantopoulos, S.H., & Moutsopoulos, H.M. (1987) Association of Metsovo lung and pleural mesothelioma with exposure to tremolite-containing whitewash. *The Lancet* **329**, 965–967.

Lee, R.J., Van Orden, D.R., Allison, K.A., & Bunker, K.L. (2009) Characterization of Airborne Amphibole Particles in Libby, MT. *Indoor Built Environment* **18**, 524–530.

Leidel, N.A., Bayer, S.G., Zumwalde, R.D., & Busch, K.A. (1979) USPSH-NIOSH membrane filter method for evaluating airborne asbestos fibers. U.S. Department of Health, Education and Welfare, NIOSH Technical Report No. **79-127**, Cincinnati, Ohio, United States.

Lentz, T., Rice, C.H., Succop, P.A., Lockey, J.E., Dement, J.M., & LeMasters, G.K. (2003) Pulmonary deposition modeling with airborne fiber exposure data: a study of workers manufacturing refractory ceramic fibers. *Applied Occupational and Environmental Hygiene* **18**, 278–288.

Lippmann, M. (2014) Toxicological and epidemiological studies on effects of airborne fibers: Coherence and public health implications. *Critical Reviews in Toxicology* **44**, 643–695.

LOWER, S.K., TADANIER, C.J., & HOCHELLA, M.F. (2000) Measuring interfacial and adhesion forces between bacteria and mineral surfaces with biological force microscopy. *Geochimica et Cosmochimica Acta* **64**, 3133–3139.

MCDONALD, J.C., MCDONALD, A.D., ARMSTRONG, B., & SEBASTIEN, P. (1986) Cohort study of mortality of vermiculite miners exposed to tremolite. *Occupational and Environmental Medicine* **61**, 436–444.

MEEKER, G.P., BERN, A.M., BROWNFIELD, I.K., LOWERS, H.A., SUTLEY, S.J., HOEFEN, T.M., & VANCE, J.S. (2003) The composition and morphology of amphiboles from the Rainey Creek Complex near Libby Montana. *American Mineralogist* **88**, 1955–1969.

MOSSMAN, B.T. (2008) Assessment of the pathogenic potential of asbestiform vs. nonasbestiform particulates (cleavage fragments in *in vitro* (cell or organ culture) models and bioassays. *Regulatory Toxicology and Pharmacology* **52**, S200–S203.

MOSSMAN, B.T., LIPPMANN, M., HESTERBERG, T.W., KELSEY, K.T., BORCHOWSKY, A., & BONNER, J.C. (2011) Pulmonary endpoints (lung carcinomas and asbestosis) following inhalation exposures to asbestos. *Journal of Toxicology and Environmental Health B* **14**, 76–121.

NATIONAL INSTITUTE FOR OCCUPATIONAL SAFETY AND HEALTH (NIOSH) (2011) Asbestos fibers and other elongate mineral particles: State of the science and roadmap for research. *Current Intelligence Bulletin* **62**, DHHS (NIOSH) Publication Number 2011-159. Center for Disease Control, Department of Health and Human Services.

PAOLETTI, L. & BRUNI, B.M. (2009) Caratterizzazione dimensionale di fibre anfiboliche new polmone e pleura di casi di mesothelioma da esposizione ambientale. *Medicina del Lavoro* **100**, 11–20.

PAOLETTI, L., BATISTI, D., BRUNO, C., DI PAOLA, M., GIANFAGNA, A., MASTRANTONIO, M., NESTI, M., & COMBA, A. (2000) Unusually high incidence of malignant pleural mesothelioma in a town of eastern Sicily: An epidemiological and environmental study. *Archives of Environmental Health* **55**, 392–398.

POOLEY, F.D. & CLARK, N. (1980) A comparison of fibre dimensions in chrysotile, crocidolite and amosite particles from sampling of airborne dust and from post mortem lung tissue. *IARC Scientific Publication* **30**, 79–86.

POOLEY, F.D. & WAGNER, J.C. (1988) The significance of the selective retention of minerals dusts. *Annals of Occupational Hygiene* **32**, 187–194.

POTT, F. (1978) Some aspects on the dosimetry of the carcinogenic potency of asbestos and other fibrous dusts. *Staub-Reinhalt Luft* **38**, 486–490.

SAKELLARIOU, K., MALAMOU-MITSI, V., HARITOU, A., KAUMPANIOU, C., STACHOULI, C., DIMOLIATIS, I.D., & CONSTANTOPOULOS, S.H. (1996) Malignant pleural mesothelioma from nonoccupational asbestos exposure in Metsovo (north-west Greece): Slow end of an epidemic? *European Respiratory Journal* **9**, 1206–1210.

SEBASTIEN, P., MCDONALD, J.C., MCDONALD, A.D., CASE, B., & HARLEY, R. (1989) Respiratory cancer in chrysotile textile and mining industries: Exposure inferences from lung analysis. *British Journal of Industrial Medicine* **46**, 180–187.

SHEDD, K.B. (1985) Fiber dimensions of crocidolite from Western Australia, Bolivia, and the Cape and Transvaal Provinces of South Africa. United States Bureau of Mines Report of Investigations **8998**.

SIEGRIST, H.G. & WYLIE, A.G. (1980) Characterizing and discriminating the shape of asbestos particles. *Environmental Research* **23**, 348–361.

SKINNER, H.C.W., ROSS, M., & FRONDEL, C. (1988) *Asbestos and other fibrous materials*. Oxford University Press, Oxford, England.

STANTON, M.F., LAYARD, M., TEGERIS, A., MILLER, E., MAY, M., MORGAN, E., & SMITH, A. (1981) Relation of particle dimensions to carcinogenicity in amphibole asbestoses and other fibrous minerals. *Journal of the National Cancer Institute* **67**, 965–975.

SULLIVAN, P.A. (2007) Vermiculite, respiratory disease, and asbestos exposure in Libby, Montana: Update of a cohort mortality study. *Environmental Health Perspectives* **115**, 579–585.

SUN, X., DRISCOLL, M.K., GUVEN, C., DAS, S., PARENT, C.A., FOURKAS, J.T., & LOSERT, W. (2015) Asymmetric nanotopography biases cytoskeletal dynamics and promotes unidirectional cell guidance. *Proceedings of the National Academy of Sciences* **112**, 12557–12562.

SUZUKI, Y. & YUEN, S.R. (2002) Asbestos Fibers contributing to the induction of human malignant mesothelioma. *Annals of the New York Academy of Sciences* **982**, 160–176.

TIMBRELL, V. (1965) The inhalation of fibrous dusts. *Annals of the New York Academy of Sciences* **132**, 255–273.

TIMBRELL, V. (1982) Deposition and Retention of Fibres in the Human Lung. *Annals of Occupational Hygiene* **26**, 347–369.

TIMBRELL, V. (1983) Fibres and carcinogenesis. *Journal of the Occupational Health Society Australia* **3**, 1–12.

TIMBRELL, V., POOLEY, F., & WAGNER, J.C. (1970) Characteristics of respirable asbestos fibres *In* Pneumoconiosis: Proceeding of the International Conference Johannesburg, 1969 (H.A. Shapiro, ed.). Oxford University Press, Cape Town, South Africa (120–125).

TIMBRELL, V., GRIFFITHS, D.M., & POOLEY, F.D. (1971) Possible biological importance of fibre diameters of South African amphiboles. *Nature* **232**, 55–56.

TIMBRELL, V., ASHCROFT, T., GOLDSTEIN, B., HEYWORTH, F., MEURMAN, L.O., RENDALL, R.E.G., REYNOLDS, J.A., SHILKIN, K.B., & WHITAKER, D. (1988) Relationships between retained amphibole fibres and fibrosis in human

lung tissue specimens. *Annals Occupational Hygiene* **32**, 323–340.

Veblen, D.R. (1980) Anthophyllite asbestos: microstructures, intergrown sheet silicates, and mechanisms of fiber formation. *American Mineralogist* **65**, 1075–1086.

Veblen, D.R. & Burnham, C.W. (1977) Asbestiform chain silicates: new minerals and structural groups. *Science* **198**, 359–365.

Veblen, D.R. & Wylie, A. (1993) Mineralogy of amphiboles and 1:1 layer silicates. *In* Health Effects of Mineral Dusts (G.D. Guthrie Jr. & B.T. Mossman, eds.). Mineralogical Society of America, Washington D.C., *Reviews in Mineralogy* **28**, 61–137.

Verkouteren, J.R. & Wylie, A.G. (2000) The Tremolite–Actinolite–Ferro-actinolite series: Systematic relationships among cell parameters, composition, optical properties, and habit and evidence of discontinuities. *American Mineralogist* **85**, 1239–1254.

Verkouteren, J.R. & Wylie, A.G. (2002) Anomalous optical properties of fibrous tremolite, actinolite and ferro-actinolite. *American Mineralogist* **87**, 1090–1095.

Vermaas, F.H.S (1952) Amphibole asbestos of South Africa. *Transactions of the Geological Society of South Africa* **55**, 199–232.

Wagner, J.C., Skidmore, J.W., Hill, R.J., & Griffiths, D.M. (1985) Erionite exposure and mesothelioma in rats. *British Journal of Cancer* **51**, 727–730.

Walker, J.S. & Zoltai, T. (1979) A comparison of asbestos fibers with synthetic crystals known a whiskers. *Annals of the New York Academy of Sciences* **330**, 687–704.

Warnock, M.L. (1989) Lung asbestos burden in shipyard and construction workers with mesothelioma: Comparison with burdens in subjects with asbestosis or lung cancer. *Environmental Research* **50**, 68–85.

Watson, M.B. (1999) *The effect of intergrowths on the properties of fibrous anthophyllite*. Master of Science Thesis, Department of Geology, University of Maryland, College Park, Maryland, United States.

White, N., Nelson, G., & Murray, J. (2008) South African experience with asbestos related environmental mesothelioma: Is asbestos fiber type important? *Regulatory Toxicology and Pharmacology* **52**, 592–596.

Williams, C., Dell, L., Adams, R., & Van Orden, D.R. (2012) State-of-the-science assessment of non-asbestos amphibole exposure: Is there a cancer risk? *Environmental Geochemistry and Health* **35**, 357–377.

Wylie, A.G. (1979) Optical properties of the fibrous amphiboles. *Annals of the New York Academy of Science* **330**, 600–605.

Wylie, A.G. (1993) Modeling asbestos populations: The fractal approach. *Canadian Mineralogist* **30**, 437–446.

Wylie, A.G. & Candela, P.A. (2015) Methodologies for determining the sources, characteristics, distribution and abundance of asbestiform and nonasbestiform amphibole and serpentine in ambient air and water. *Journal of Toxicology and Environmental Health Part B Critical Reviews* **18**, 1–42.

Wylie, A.G. & Schweitzer, P. (1982) The effects of sample preparation on size and shape of mineral particles: The case of wollastonite. *Environmental Research* **27**, 52–73.

Wylie, A.G. & Verkouteren, J.R. (2000) Amphibole asbestos from Libby, Montana: Aspects of nomenclature. *American Mineralogist* **85**, 1540–1542.

Wylie, A.G. & Virta, R.L. (2015a) Size and shape characteristics of mountain-leather actinolite. Digital Repository at the University of Maryland, http://dx.doi.org/10.13016/M2WT68.

Wylie, A.G. & Virta, R.L. (2015b) Size and shape characteristics of South African actinolite asbestos (ferro-actinolite): Digital Repository at the University of Maryland, http://dx.doi.org/10.13016/M2S138.

Wylie, A.G. & Virta, R.L. (2016a) Size and shape characteristics of Indian tremolite asbestos: Digital Repository at the University of Maryland, http://dx.doi.org/10.13016/M21H7S.

Wylie, A.G. & Virta, R.L. (2016b) Size distribution measurements of amosite, crocidolite, chrysotile, and nonfibrous tremolite. Digital Repository at the University of Maryland, http://dx.doi.org/10.13016/M2798Z.

Wylie, A.G., Bailey, K.F., Kelse, J.W., & Lee, R.J. (1993) The importance of width in asbestos fiber carcinogenicity and its implications for public policy. *American Industrial Hygiene Association Journal* **54**, 239–252.

Wylie, A.G., Skinner, H.C.W., Marsh, J., Snyder, H., Garzione, C., Hodkinson, D., Winters, R., & Mossman, B.T. (1997) Mineralogical features associated with cytotoxic and proliferative effects of fibrous talc and asbestos on rodent tracheal epithelial and pleural mesothelial cells. *Toxicology and Applied Pharmacology* **147**, 143–150.

Wylie, A.G., Schweitzer, P., & Siegrist, H.G. (2015) Size and shape characteristics of amphibole cleavage fragments from milled riebeckite. Digital Repository at the University of Maryland, http://dx.doi.org/10.13016/M2S98X.

Wylie, A.G., Virta, R.L., Shedd, K.B., & Snyder, J.G. (2015) Size and shape characteristics of airborne amphibole asbestos and amphibole cleavage fragments. Digital Repository at the University of Maryland, http://dx.doi.org/10.13016/M2HP87.

Yaziciogly, S., Ilcayto, R., Balci, K., Sayli, B.S., & Yorulmaz, B. (1980) Pleural calcification, pleural mesotheliomas, and bronchial cancers caused by tremolite dust. *Thorax* **35**, 564–569.

Received December 13, 2015. Revised manuscript accepted May 5, 2016.